

FREE VOLUME EFFECTS IN POLYMER SOLUTIONS

by

Daniel Gaeckle

A Thesis Submitted to the Faculty of Graduate
Studies and Research in Partial Fulfilment of the
Requirements for the Degree of Doctor of Philosophy

Department of Chemistry
McGill University
Montreal, Quebec, Canada

May 1972

To My Wife Chantal

FREE VOLUME EFFECTS IN POLYMER SOLUTIONS

ABSTRACT

The effect of pressure on polymer solution properties has been investigated by light scattering. Second virial coefficients, A_2 , and radii of gyration, $\langle S^2 \rangle^{1/2}$, were determined at high polymer dilution, at different temperatures and pressures, for polyisobutylene in 2-methylbutane and polystyrene in 2-butanone. The pressure and temperature dependences of A_2 were found consistent with newer "free volume" theories of polymer solution thermodynamics, and were used to obtain relative partial molar volumes, $\Delta\bar{V}_1$, and heats, $\Delta\bar{H}_1$. A correlation between values of $\langle S^2 \rangle^{1/2}$ and A_2 shows that pressure influences these quantities through its effect on the interaction χ parameter or on the z parameter.

The UCST pressure dependence was investigated in various polymeric systems. Even for non-solvent systems, such as polystyrene in n-alkanes, the free volume manifests its presence in the UCST region.

Heats of dilution, $\Delta\bar{H}_1$, were determined calorimetrically at 25° for five polystyrene-solvent systems. These data were used to analyze the Flory theory, which fails to predict the experimental results when the free volume effects are predominant.

Orientational effects have been investigated in long chain n-alkanes mixtures with carbon tetrachloride, in order to elucidate the failure of the corresponding states principle, as applied to polymer solutions.

ACKNOWLEDGEMENTS

I wish to express my sincere gratitude to Professor D. Patterson for his interest, constant encouragement and guidance during the course of this work and his assistance in preparing this thesis.

Thanks are also due to:

Professor G. Delmas Patterson of the Université du Québec, for use of the CRMT calorimeter.

Professor M. Rinfret of the Université de Montréal, for use of his equipment.

McGill University, The Xerox Company, the Paint Research Institute and the National Research Council of Canada for financial assistance.

TABLE OF CONTENTS

	<u>Page</u>
ABSTRACT	
ACKNOWLEDGEMENTS	i
TABLE OF CONTENTS	ii
LIST OF FIGURES	iv
LIST OF TABLES	vi
LIST OF SYMBOLS	vii
1. INTRODUCTION	1
2. ROLE OF PRESSURE IN POLYMER SOLUTION THERMODYNAMICS	9
2.1 EFFECT OF PRESSURE ON THE SECOND VIRIAL COEFFICIENT AND CHAIN DIMENSIONS IN POLYMER SOLUTIONS	9
2.1.1 Thermodynamic Considerations	10
2.1.2 Experimental	14
2.1.3 Results and Discussion	29
2.2 EFFECT OF PRESSURE ON PHASE BOUNDARIES	41
2.2.1 Experimental	44
2.2.2 Results and Discussion	47
3. HEATS OF DILUTION OF POLYMER SOLUTIONS	56
3.1 THE HEATS OF DILUTION IN POLYSTYRENE SOLUTIONS	57
3.1.1 Experimental	59
3.1.2 Results	68
3.1.3 Discussion	76

	<u>Page</u>
3.2 THE HEATS OF MIXING OF LOW MOLECULAR WEIGHT COMPOUND MIXTURES	86
3.2.1 Experimental	86
3.2.2 Results and Discussion	92
3.3 GENERAL CONCLUSIONS	105
4. CONTRIBUTIONS TO ORIGINAL KNOWLEDGE AND SUGGESTIONS FOR FURTHER WORK	107
REFERENCES	111
APPENDIX	A1

LIST OF FIGURES

<u>Figure</u>		<u>Page</u>
1	Flow Chart of the Pressure System	19
2	The Refractive Index as a Function of Concentration for PIB+2-Methylbutane	23
3	The Second Virial Coefficient, A_2 , as a Function of Pressure for PIB+2-Methylbutane and PS+2-Butanone	27
4	The Radius of Gyration, $\langle S^2 \rangle^{\frac{1}{2}}$, as a Function of Pressure for PIB+2-Methylbutane and PS+2-Butanone	28
5	The Coil Expansion Factor, α , for the Polymer-Solvent Systems at Various Pressures and Temperatures, as a Function of $zh(z)$	38
6	Zimm Plot for PS+2-Butanone at 22° and Atmospheric Pressure	42
7	Berry Plot for PS+2-Butanone at 22° and Atmospheric Pressure	43
8	(P,T) Cloud Point Curves for a PS Fraction of Molecular Weight 2030 in Alkanes	51
9	Critical Lines in Reduced Pressure and Temperature Co-ordinates	52
10	The Shultz-Flory Plot for PS+Hexane	54

<u>Figure</u>		<u>Page</u>
11	A Cross Section View of the Calorimeter Cell	62
12	Experimental Set-Up for Calibrations	62
13	The Enthalpy Parameter, χ_H , as a Function of the Segment Fraction, ϕ_2 , for PS+Cyclohexane, +Cyclopentane, and +2-Butanone, at 25°	69
14	The Enthalpy Parameter, χ_H , as a Function of the Segment Fraction, ϕ_2 , for PS+Toluene, +Ethylbenzene, and PIB+n-Pentane, at 25°	70
15	The Heat of Mixing of Cyclohexane+n-Hexane per mole as a Function of the Molar Fraction of Cyclohexane at 25°	93
16	The Heat of Mixing per Unit "Hard Core" Volume, $\Delta H/x_1V_1^* + x_2V_2^*$, as a Function of the Segment Fraction of 2,2,4,4,6,8,8-Heptamethylnonane in a n-Pentane at 25°	94
17	The Heat of Mixing per Unit "Hard Core" Volume, $\Delta H/x_1V_1^* + x_2V_2^*$, as a Function of the Segment Fraction, ϕ_2 , of the Alkane, at 25° for CCl ₄ + 2,2-Dimethylbutane, +n-Hexane, and CCl ₄ +2,2,4-Trimethylpentane, +n-Octane	101
18	The Heat of Mixing per Unit "Hard Core" Volume, $\Delta H/x_1V_1^* + x_2V_2^*$, as a Function of the Segment Fraction, ϕ_2 , of the Alkane, at 25°, for CCl ₄ + 2,2,4,4,6,8,8-Heptamethylnonane, +n-Hexadecane and Benzene+2,2,4,4,6,8,8-Heptamethylnonane, +n-Hexadecane	102

LIST OF TABLES

<u>Table</u>		<u>Page</u>
1	Refractive Index Increments for PIB+2-Methylbutane	25
2	Refractive Index Increments for PS+2-Butanone	25
3	Equation of State Parameters for PIB+2-Methylbutane	34
4	Values of the Slope of the Critical Lines, $(dP/dT)_c$, at Zero Pressure for PS Systems	55
5	Tian-Calvet Differential Calorimeter Calibration Constants at 25°	66
6	Calculated χ , χ_H , χ_S at 25° According to the Flory Theory	73
7	Pure Component and Solution Parameters at 25°	75
8	Origin and Specifications of the Liquids Used for the Heats of Mixing Experiments	87
9	Calibration Constants of CRMT Calorimeter at 25°	91
10	Pure Component Parameters at 25°	95
11	Experimental Data and Calculated Parameters for the System 2,2,4,4,6,8,8-Heptamethylnonane+n-Pentane at 25°	97
12	Experimental Data and Calculated Parameters at 25°	98

LIST OF SYMBOLS

A	excluded volume theory parameter
A_2	second virial coefficient in dilute solution
A_2^{conc}	second virial coefficient in concentrated solution
B	excluded volume theory parameter
C_p	configurational heat capacity
ΔG_H	Gibbs free energy of mixing
H^E	excess enthalpy
ΔH_d	experimental value of the heat of dilution
ΔH_M	enthalpy of mixing
$\Delta \bar{H}_1$	enthalpy (or heat) of dilution
I	scattered intensity
I	current
I_B^{25}	scattered intensity at 90° angle, 25° , by the reference system
$\langle L^2 \rangle^{\frac{1}{2}}$	mean end-to-end distance
LCST	lower critical solution temperature
M	molecular weight
N_A	Avogadro's number
P	pressure
Q_w^i	polydispersity correction parameter
R	gas constant

S	molecular surface of a molecule or of a polymer segment
S^E	excess entropy
ΔS_M	entropy of mixing
$\langle S^2 \rangle^{\frac{1}{2}}$	radius of gyration
T	temperature
T_g	glass temperature
U	configurational energy
UCST	upper critical solution temperature
V	volume
V^E	excess volume
ΔV_M	volume of mixing
$\Delta \bar{V}_1$	volume of dilution or relative partial molar volume
X_{12}	contact interaction parameter
c	concentration, g/cm ³
c_i	degree of freedom
h	polydispersity factor
$h(z)$	excluded volume function
k	Boltzmann's constant
k_V	volume of dilution parameter
n	refractive index
Δn_1	number of mole of component 1 added
q_s	polydispersity correction factor

r	volume fraction
s_i	surface to volume ratio of component i
$v_{sp,i}$	specific volume of component i
Δw	interchange energy
w_i	weight of component i
w_{ij}	i - j contact energy
x	mole fraction
z	excluded volume parameter
z	lattice co-ordination number
χ	polymer-solvent interaction parameter
χ_H	enthalpy parameter
$\chi_{H,app}$	apparent enthalpy parameter
$\chi_{H,i}$	i th term in the series expansion of χ_H as a function of segment fraction
χ_S	entropy parameter
ψ	entropy parameter (former Flory-Huggins theory)
ψ	excluded volume function
α	coil expansion factor
α_i	thermal expansion coefficient of component i
β_i	isothermal compressibility of component i
ϕ_i	segment fraction of component i

ϕ_i	volume fraction of component i
ϕ_i^f	final segment fraction of component i
ϕ_i^i	initial segment fraction of component i
ϕ_i^a	mean segment fraction of component i
λ	wavelength
$\Delta\mu_i$	change in chemical potential of component i
γ	"chemical difference" parameter
π	free volume theory parameter
π	osmotic pressure
ρ	parameter in the KCKR theory
ρ_i	density of component i, g/cm ³
τ	structural parameter in the free volume theory
θ	Theta temperature
θ	angle between the incident and the scattered beams
θ_i	surface fraction of component i

Superscripts

*	reduction parameter
~	reduced quantity

Subscripts

0	Theta state
1	solvent
2	solute

c	critical state
n	number average
v	viscosity average
w	weight average
z	z-average
i	component i

1. INTRODUCTION

An interest in polymer solutions and their properties has always played a key role in polymer science. Indeed, the existence of macromolecules was demonstrated through work on solution viscosities by Staudinger in the 1920's. Turning to the thermodynamics of polymer solutions, most of the fundamental concepts have their origin in theories of mixtures of small molecules, which for the sake of clarity, will be mentioned here.

In the theory of strictly regular solutions^{1,2} of small molecules, the ideal solution (following by definition Raoult's law) plays the role of a reference system defining excess thermodynamic quantities such as H^E , S^E . The model on which the theory is based, requires a few basic hypotheses, but only one has direct bearing on subsequent remarks. This is the assumption of a rigid lattice for the solution which does not allow any change of volume during the mixing process and where each molecule occupies only one lattice site. The main consequence of this is that the excess entropy, S^E , is zero and any deviation from ideality ought to be enthalpic in nature.

Following K.H. Meyer, Flory³ and Huggins⁴ independently used statistical mechanics methods and the lattice model to give an expression for the combinatorial entropy of mixing of polymer solutions. But now the solution is made of two species of different molecular dimensions. The polymer and

the solvent are to be divided into equal-sized quasi-spherical segments, each occupying one lattice site. Again use of the lattice model is made for the calculation of the heat of mixing. This approach, taken from the strictly regular solution theory, is now applied to the mixture of polymer and solvent segments. The interaction parameter χ is given by

$$\chi = z\Delta w/kT \quad (1)$$

if the solvent is monomeric. The parameter z is the coordination number, introduced by the lattice model and Δw is the interchange energy, associated with the formation of unlike (1-2) contacts from like (1-1) and (2-2) contacts, according to a quasi-chemical equation. Therefore:

$$\Delta w = \frac{1}{2} (w_{11} + w_{22}) - w_{12} \quad (2)$$

Here w_{ij} are "contact energies" associated with the energy required to break an ij contact. For non-polar systems, w_{12} may be approximated by the geometric mean rule, which by substitution in eq.(2) yields:

$$\Delta w = \frac{1}{2} (w_{11}^{\frac{1}{2}} - w_{22}^{\frac{1}{2}})^2 \quad (3)$$

The χ parameter is the endothermic energy change necessary for the formation of the (1-2) contacts, divided by the thermal energy kT . It is thus a measure of polymer-solvent "antipathy".

Later Flory⁵, following Guggenheim's work⁶ on small molecules, assumed that Δw in eq.(1) (and hence χ) has the character of a free energy. As a result, the solubility parameter is then the sum of an enthalpic and entropic term:

$$\chi = \chi_H + \chi_S = \kappa + \frac{1}{2} - \psi \quad (4)$$

(Two different nomenclatures have been used in the past. The quantities χ_H and κ are equivalent as are χ_S and $\frac{1}{2} - \psi$). However, that modification was not sufficient to account for some disturbing experimental facts.

Freeman and Rowlinson⁷ in 1959 found that polymer solutions separate into two phases on increasing the temperature to what is called the lower critical solution temperature or LCST. Thus, polymer solutions presenting both an upper critical solution temperature or UCST (associated with the Flory theta temperature) and an LCST, can not be described by the function given in eq.(1), which decreases monotonically with temperature. Moreover, traditional theories based on energetic concepts can not explain, even qualitatively, the negative heats of solutions^{8,9} which have been found even at room temperatures. The heat of mixing is indeed proportional to Δw , which, according to eq.(3), is always positive for non-polar systems.

One can visualize in a simple qualitative way what is happening at the LCST. The phase separation would be predicted if ΔG_M is positive:

$$\Delta G_M = \Delta H_M - T \Delta S_M \quad (5)$$

However, ΔH_M , according to thermodynamics, has to be negative if phase separation occurs upon increasing the temperature. Therefore, at the LCST, the enthalpic contribution to ΔG_M favours dissolution and it is a negative entropic term which renders ΔG_M positive and causes phase separation.

These two observations, LCST and negative heats, can be explained if the volume of mixing is no longer neglected. The new factor which accounts for the change is the free volume concept, that is the excess of the volume a molecule occupies in the liquid at any given temperature, over its volume, labelled "hard core", at 0 K. Recent work^{10,11} in polymer solution thermodynamics shows the importance of a difference of free volumes, or degrees of thermal expansion, between the polymer and the solvent. During the mixing process, the free volumes move towards an intermediate value characteristic of the mixture. These changes produce major contributions (termed structural¹⁰ or equation of state¹¹) to the thermodynamic mixing functions, ΔH_M , ΔS_M and ΔG_M as well as ΔV_M . The free volume contribution to ΔG_M and the interaction parameter, χ , is pre-

dicted to be positive. It accounts¹² for the existence of the lower critical solution temperature occurring in polymer solutions at high temperature, where there is a large difference in free volume between polymer and solvent. The importance of free volume suggests that pressure should be as important a thermodynamic variable as temperature. The application of pressure will normally compress the solvent to a much greater extent than the polymer, thus reducing the free volume difference between them, and also the corresponding contribution to ΔG_M and χ . Pressure does in fact markedly increase¹³ the value of the LCST, with a corresponding enhancement of polymer solubility. It is evident that pressure should have a large effect on quantities which reflect the polymer-solvent interaction, in particular the second virial coefficient, A_2 , and the radius of gyration of the macromolecule, $\langle S^2 \rangle^{\frac{1}{2}}$. Where the free volume contribution is dominant, i.e. at higher temperatures or in systems where the disparity of intermolecular forces between the polymer and solvent is small, A_2 and $\langle S^2 \rangle^{\frac{1}{2}}$ should increase with pressure. This would correspond to a decrease of ΔG_M , or to a negative value of ΔV_M . At low temperature, however, approaching the upper critical solution temperature, the free volume contribution may be of less importance. Then the second virial coefficient and the polymer dimensions could be increased or decreased with pressure, corresponding to, respectively, negative or positive values of

ΔV_M . However pressure, as a means of changing thermodynamic properties of a polymer solution, has been little used, and therefore should be an interesting tool, complementary to temperature, for exploring A_2 and $\langle S^2 \rangle^{\frac{1}{2}}$.

We have seen in the foregoing review of various theories that the crucial step, in going from the classical lattice theory to the newer ones, was to get rid of the lattice model "rigidity" and take temperature, pressure and composition changes into account, leading to thermodynamic parameters which are dependent on these variables. Temperature and pressure dependences have already been dealt with, but the concentration dependence of χ is clearly a new factor in the free volume theories. The Flory-Huggins treatment merely stated that the interaction parameter χ was not concentration-dependent.

Eichinger and Flory^{14b-d}, Flory et al.^{15,16,17} have used the "new" Flory theory to treat thermodynamic data for polyisobutylene and polystyrene solutions. The predicted concentration dependence of the thermodynamic functions is generated by fitting the theory to experimental heats of mixing of the polymer in the solvent at infinite dilution. However, agreement between theory and experiment is only fair, and further experimental tests are in order. The largest predicted variations of a thermodynamic parameter occurs for χ_H , the enthalpy parameter. Direct determinations of χ_H by calorimetry

are almost non-existent, particularly when χ_H is negative, corresponding to an important free volume effect. A full test of the theory has not been possible for this reason.

The purpose of this work is to test the free volume theories.

1. A quantitative investigation of the second virial coefficient, A_2 , and polymer chain dimensions, $\langle S^2 \rangle^{1/2}$, dependences on pressure was carried out by a photometric method, under experimental conditions where the free volume effect is prominent. Our interest however, was not confined to the phase separation region. Light scattering is indeed a powerful method to determine solution properties over a wide range of temperature and pressure. The polyisobutylene (PIB) + 2-methylbutane system was investigated at temperatures below and above the LCST at different pressures, providing, en passant, some knowledge about the LCST phase boundary. The second system studied with this technique, polystyrene (PS) + 2-butanone has an excess volume V^E large in magnitude and should therefore show an important change in free enthalpy of mixing as pressure is varied.

In addition, a more qualitative and systematic study of the pressure dependence of the UCST has been performed on different polymer-solvent systems. This section of

our work was intended to show the role of free volume, as derived from phase equilibria analysis, in conditions where the free volume contribution is of less importance.

2. Heats of dilution will be obtained for polymer-solvent systems showing the effect of the free volume dissimilarity between the two components. In the course of this work, it appeared necessary to measure heats of mixing of low molecular weight model compounds.

2. ROLE OF PRESSURE IN POLYMER SOLUTION
THERMODYNAMICS

2.1 EFFECT OF PRESSURE ON THE SECOND VIRIAL COEFFICIENT AND CHAIN DIMENSIONS IN POLYMER SOLUTIONS

Schulz and Lechner¹⁸⁻²⁰ have pioneered in the study of the effect of pressure on light scattering in polymer solutions. Using a high pressure optical cell and special instrumentation they have made measurements up to 800 atm and at various temperatures on a number of systems: polystyrene+trans-decalin, +toluene, +cyclohexane and +chloroform. The results have been shown to be in qualitative and semi-quantitative agreement with a theoretical treatment²¹ of pressure effects. In particular, $(\partial A_2/\partial P)_T$ for polystyrene+trans-decalin^{18,19} is negative near the UCST ($\theta = 19^\circ$), that is $\Delta V_M > 0$. However, at higher temperature, $(\partial A_2/\partial P)_T$ becomes positive (for small pressures) indicating that $\Delta V_M < 0$. More recently, Wolf²², using the Schulz-Lechner instrumentation and technique, studied the PIB +pentane and PIB +iso-octane systems, for which the interactions should only be of a free volume nature. The present work is an investigation of PIB + 2-methylbutane and PS + 2-butanone at lower pressure, using the standard SOFICA light scattering equipment, and with new features of interpretation.

2.1.1 Thermodynamic Considerations

Relationship between the pressure and temperature dependence of A_2 and volumes and heats of dilution at low concentration.

The following standard relation is valid at low concentration:

$$\frac{\Delta\mu_1}{RT} = -\frac{\pi V_1}{RT} = \frac{cV_1}{M} + A_2 c^2 V_1 \quad (6)$$

Here $\Delta\mu_1$ is the difference between the chemical potential of the solvent in the solution and in the pure liquid, and π is the osmotic pressure. V_1 is the molar volume of the pure solvent at the experimental temperature and pressure and c is the usual concentration, i.e. weight of polymer/volume of solution. The relative partial molar volumes and enthalpies of the solvent (volumes and heats of dilution), $\Delta\bar{V}_1$, and $\Delta\bar{H}_1$ are obtained through the pressure and temperature dependences of A_2 at constant weight fraction, w_2 , or mole fraction, rather than constant concentration. We have, at low concentration:

$$\frac{\Delta\bar{V}_1}{V_1} = \frac{1}{V_1} \left[\frac{\partial(\pi V_1)}{\partial P} \right]_{T, w_2} = c^2 RT \left[- \left(\frac{\partial A_2}{\partial P} \right)_T - \beta_1 A_2 \right] \quad (7)$$

$$\frac{\Delta\bar{H}_1}{RT} = T \left[\frac{\partial(\pi V_1/RT)}{\partial T} \right]_{P, w_2} = c^2 V_1 T \left[\left(\frac{\partial A_2}{\partial T} \right)_P - \alpha_1 A_2 \right] \quad (8)$$

Here β_1 and α_1 are the isothermal compressibility and the thermal expansion coefficient, or thermal expansivity, of the solvent. In the present work, the terms in β_1 and α_1 are negligible compared with the pressure and temperature variation of A_2 . Equation (8) for $\Delta\bar{H}_1$ has been given by Schulz and Lechner^{18,19}. Their expression for $\Delta\bar{V}_1$, however, is apparently incorrect, and would give infinite values as $P \rightarrow 0$. An error was incurred through equating energy changes at constant pressure and volume in their¹⁹ eq. (9).

Comparison of relative partial molar heats and volumes of the solvent in dilute and concentrated solution.

Equations (7) and (8) give the $\Delta\bar{V}_1$ and $\Delta\bar{H}_1$ in the dilute region where the solution is non-uniform due to the excluded volume effect. These values presumably cannot be directly compared with the usual heat and volume measurements made at higher concentrations where the polymer molecules interpenetrate and the solution is uniform. In dilute solution theories, solution non-uniformity gives rise to the $h(z)$ function in the A_2 expression²³:

$$A_2 = \frac{1}{2} N_A B h(z) = 1.52 N_A A^3 M^{-1/2} z h(z) \quad (9)$$

where B and z are the long-range, polymer-solvent interaction parameters²³:

$$B = 2 \left(\frac{1}{2} - \chi \right) / N_A V_1 \rho^2 \quad (10)$$

$$z = 0.330 B M^{1/2} / A^3 \quad (11)$$

and

$$A = \left(\langle L_0^2 \rangle / M \right)^{1/2} \quad (12)$$

The quantities ρ and $\langle L_0^2 \rangle$ are respectively the density of the polymer and the mean-square unperturbed end-to-end distance of the macromolecule. Direct thermodynamic measurements of volumes and heats of mixing leading to values of $\Delta \bar{V}_1$ and $\Delta \bar{H}_1$ are usually made at high concentrations, between 20 and 80% of polymer. Equations (7) and (8) could be used to predict these values of $\Delta \bar{V}_1$ and $\Delta \bar{H}_1$ if values of A_2 were available for high polymer concentration (A_2^{conc}). At a sufficiently high concentration, which is probably no more than $\sim 5\%$, the theoretical expression for A_2 still corresponds to eq. (9), but the excluded volume function $h(z)$ is absent. We therefore obtain A_2^{conc} for use in eqs. (7) and (8) from experimental dilute solution values of A_2 through division by $h(z)$, i.e.

$$A_2^{\text{conc}} = A_2 / h(z) \quad (13)$$

In work in the concentrated range, the traditional composition variable has been the volume fraction ϕ_2' , related to the concentration by:

$$\lim_{c \rightarrow 0} (\phi_2'/c) = v_{2,sp} \quad (14)$$

where $v_{2,sp}$ is the specific volume of the pure polymer. It has been usual to obtain the volume of mixing, ΔV_M , rather than $\Delta \bar{V}_1$, and it is found that ΔV_M is symmetrical in the volume fractions of the components, i.e.²⁴

$$\Delta V_M/V = k_V \phi_1' \phi_2' \quad (15)$$

leading to

$$\Delta \bar{V}_1/V_1 = k_V \phi_2'^2 \quad (16)$$

Similarly the heat of dilution is given by

$$\Delta \bar{H}_1/RT = \chi_H \phi_2'^2 \quad (17)$$

Combining eqs. (7) and (8) with (16) and (17), we have

$$k_V = \frac{RT}{v_{2,sp}^2} \left[- \left(\frac{\partial A_2^{\text{conc}}}{\partial P} \right)_T - \beta_1 A_2^{\text{conc}} \right] \quad (18)$$

$$\chi_H = \frac{V_1 T}{v_{2,sp}^2} \left[+ \left(\frac{\partial A_2^{\text{conc}}}{\partial T} \right)_P - \alpha_1 A_2^{\text{conc}} \right] \quad (19)$$

Recently the segment fraction (designated here as ϕ_2) has been used¹¹ as a composition variable. Then

$$\lim_{c \rightarrow 0} (\phi_2/c) = v_{2,sp} \tilde{V}_2/\tilde{V}_1 \quad (20)$$

where the \tilde{V} are the reduced volumes of the pure components. Values of χ_H found in terms of the segment fractions are then given by

$$\begin{aligned} \chi_H(\text{segment fraction})/\chi_H(\text{volume fraction}) \\ = (\tilde{V}_2/\tilde{V}_1)^2 \end{aligned} \quad (21)$$

2.1.2 Experimental

2.1.2.1 Materials

Light scattering gave an M_w value of 1.02×10^6 for the Esso Vistanex PIB fraction which we used while $M_w/M_n = 1.45$ from gel permeation chromatography. The polystyrene fraction was from Pressure Chemical Co. (Pittsburgh, Pa.) with a nominal molecular weight of 8.6×10^5 and an M_w/M_n value given as less than 1.15. Our value of M_w , determined by light scattering, was 9.75×10^5 , and a determination by gel permeation chromatography was consistent with this value. Values of $M_z/M_w \sim 1.10$ have been obtained²⁵ for the series of Pressure Chemical Co. polystyrene fractions. They are thus very sharp. The 2-methyl-

butane was Phillips "pure grade" (99.0% pure), and the 2-butanone was a Fisher Certified Reagent. Both solvents were subjected to column fractionation. The purity of the 2-butanone was tested by gas liquid chromatography and impurities were found to be less than 0.1%.

2.1.2.2 The Photometer

The photogonioidiffusometer used is a commercial model (type 42000), manufactured by the Société Française de Contrôle et d'Analyse (SOFICA). A brief description of the instrument, designed by Wippler and Scheibling²⁶, will be given, emphasizing only the most critical features.

The light source is a vapour mercury lamp (SP 500 Phillips). A condenser lens gives an image of the source in the plane of an adjustable slit, acting as a diaphragm. The incident beam, of rectangular section (2 mm x 10 mm) is focused on to the entry face of the cell. The incident beam enters a vat filled with toluene (in our case) surrounding the measuring cell. A light trap on the wall of the vat absorbs the incident light at the exit of the measuring cell. A Wratten filter 61 isolates the green line ($5461 \overset{\circ}{\text{A}}$). This set-up for the incident beam has several advantages:

- intense light source.
- the collimation system defines an almost rectangular beam (the maximum convergence angle being $1^{\circ}30$).

- the intensity of the beam can be adjusted continuously.
- minimization of stray light due to reflections and refractions at interfaces (the toluene has about the same refraction index as glass) and convenient temperature regulation.

The optical system of the scattered beam is integrated in a mobile platform round the axis of the measuring cell. Two slits of 2 mm x 10 mm define the dimensions of the beam which is received on a photomultiplier RCA 1P28 (9 stages) of low dark current. The photoelectric current is measured by a shock-proof and antivibrating galvanometer (SEFRAM) having a maximum sensitivity of 10^{-9} A/mm. The high voltage required by the photomultiplier (about 800 volts) is supplied by a special unit incorporated in the instrument and stabilized to better than 0.05%. Besides, the power supply of the instrument is fed through a voltage-regulator in order to minimize the fluctuations of the incident light intensity. Nonetheless these fluctuations do exist to a certain extent and are overcome in the following way. A small portion of the incident beam is scattered on to a reference photocell, the output of which is used to vary the voltage of the measuring photomultiplier. Thus the intensity variations of the light source are compensated and can be controlled on the voltmeter dial.

2.1.2.3 The Cells

The cells supplied by the manufacturer can be used with non-volatile solvents only, at room temperature and atmospheric pressure. They are cylindrical in shape, made of thin wall glass (approximately 1 mm thick) and have a stainless steel cover. Their capacity is about 20 cm³.

The cells used at higher pressures and/or temperatures close to or above the normal boiling point of the solvent were designed such that the photometer could be used without modification. They are a compromise of optical quality and mechanical strength (internal pressure). The middle section of such a cell is made from heavy wall Pyrex tubing, 38 mm in length and 19 mm O.D. The top and bottom parts, made of stainless steel (Reno Micro Precision Engrg., Montreal) are held tightly together by means of four screws. The metal-glass seal is provided by a Teflon o-ring, underneath which a rubber o-ring was placed, to provide some elasticity while putting the cell together. The top of the cell is connected to the pressure line.

These "pressure cells", cut from ordinary Pyrex tubing, had, even after severe screening, imperfections on the surface and internal tensions as well, which may give rise to birefringence. Moreover, the thickness of the glass wall (about 3.5 mm) should yield some stray scattering. Only the cells performing like the thin wall SOFICA cells were retained:

two out of a batch of thirty-five fulfilled the criteria. Nonetheless, a correction factor was taken into account.

2.1.2.4 The Pressure Equipment

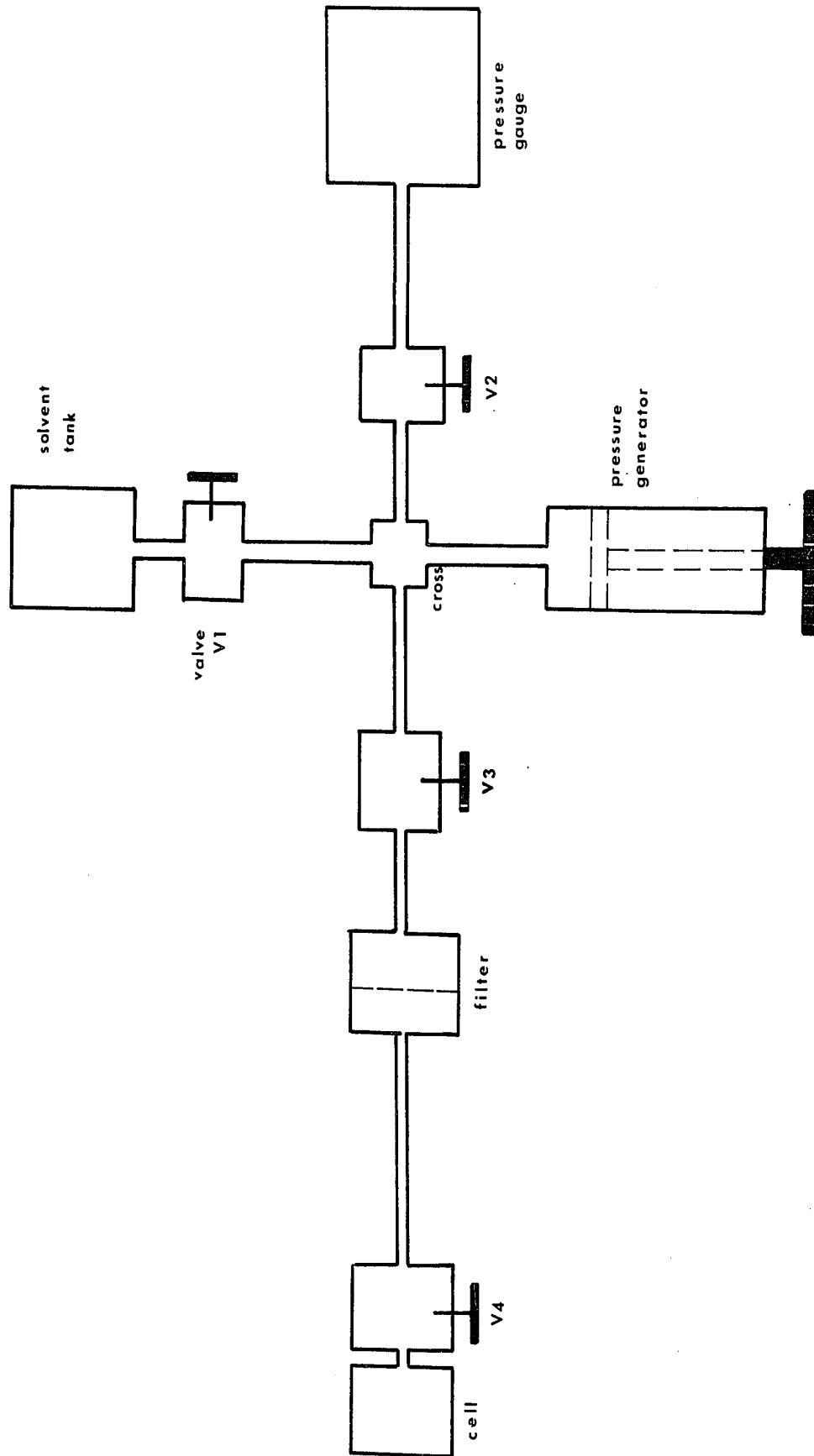
A brief description of the set-up used for generating the pressure is given in Figure 1. The pressure generator (High Pressure Co., Erie, Pa.), acting like a piston on a small volume of liquid (the capacity is 20 cm^3), is manually driven. The solid-front pressure gauge (Heise Bourdon Tube Co., Newton, Conn.) had been factory calibrated at every 40 bars up to 800 bars at 20° . The resolution is of the order of 0.5 bar. The high pressure filter (Millipore) has a porosity of 0.45μ . The whole installation, including the **four** two-way valves and the tubing (Autoclave Engineers, Erie, Pa.) was made of stainless steel. The connections were all of AE cone type.

2.1.2.5 Procedure

Prior to an experiment, the whole glassware, including the cell, was immersed for at least 24 hours in sulfochromic acid, then thoroughly rinsed with distilled water and dried. Next the material was flushed continuously with solvent in a siphon-type refluxer. Finally, a few hours before the experiment, the glassware was dried in a vacuum oven.

FIGURE 1

FLOW CHART OF THE PRESSURE SYSTEM



The pressure system was filled completely with the solvent used for the light scattering measurement. This liquid constituted the pressure medium.

The polymer solution, of known concentration, was cleared of dust by centrifugation at 25,000 g, in a Spinco centrifuge, for about $1\frac{1}{2}$ hour at -10° . The centrifuge cells, made of stainless steel, had a capacity of about 9 cm^3 and were tightly capped; usually for each solution three cells had to be run to make up the required quantity. Then the solution was transferred into the measuring cell. Each step was carried out in a refrigerated room (the temperature was about 1° to 2°) to avoid any change in concentration. The solution, due to its own thermal expansion coefficient, will fill in the space from the cell to the valve V4. This valve was always kept closed except for letting in solvent to raise the pressure. Thus the value of the concentration did not change.

Light intensities obtained with the pressure cell were corrected by comparison with those obtained using a conventional cell furnished with the instrument. This was done at each concentration of the system and for each angle of measurement. The corrections to the light intensity, established at room temperature and atmospheric pressure, did not exceed 5%, and were used at other temperatures and pressures. A benzene standard was used for calibration at each temperature, in the manner described in reference 27. The "benzene"

standard, supplied by SOFICA, is made of special glass and was used as a secondary reference, the ratio of the intensity scattered by the benzene standard over the intensity scattered by pure benzene at a 90° angle being equal to 0.9.

The angle-dependence technique (Zimm plot), as shown in Figure 6, was employed for the determination of M_w , A_2 and $\langle S^2 \rangle^{1/2}$. The intensities of scattered light of $\lambda = 5461 \text{ \AA}$ were measured at seven angles from 45° to 135° and at six concentrations ranging from 3×10^{-4} to $30 \times 10^{-4} \text{ g/cm}^3$. The equation used for obtaining M_w and A_2 was²⁷

$$0.506 I_B^{25} \left(\frac{dn}{dc} \right)^2 \left(\frac{c}{l} \right)_{\substack{\theta=0 \\ c \rightarrow 0}} = \frac{1}{M_w} + 2A_2 c \quad (22)$$

based on a value of the Rayleigh Ratio for benzene at 25° , $R_B = 16.3 \times 10^{-6}$ for $\lambda = 5461 \text{ \AA}$. I_B^{25} is the scattered intensity for the benzene standard at 25° and at a 90° angle, while dn/dc is the refractive index increment at the experimental temperature and pressure.

The radius of gyration was found in the usual manner from the ratio of the slope of $(c/l)_{\substack{\theta=0 \\ c=0}}$ to the intercept of c/l at zero concentration and angle:

$$\langle S^2 \rangle^{1/2} = \frac{\sqrt{3}\lambda}{4\pi n} \left[\text{slope } \left(\frac{c}{I} \right)_{\theta=0} / \left(\frac{c}{I} \right)_{\theta=0} \right]^{1/2} \quad (23)$$

We have also used the modified procedure, due to Berry²⁸, in which $(c/I)^{1/2}$ is plotted against $\sin^2 \frac{\theta}{2}$ and c (see Figure 7). The results for M_w , A_2 and $\langle S^2 \rangle^{1/2}$ are very similar to those obtained with the Zimm plot.

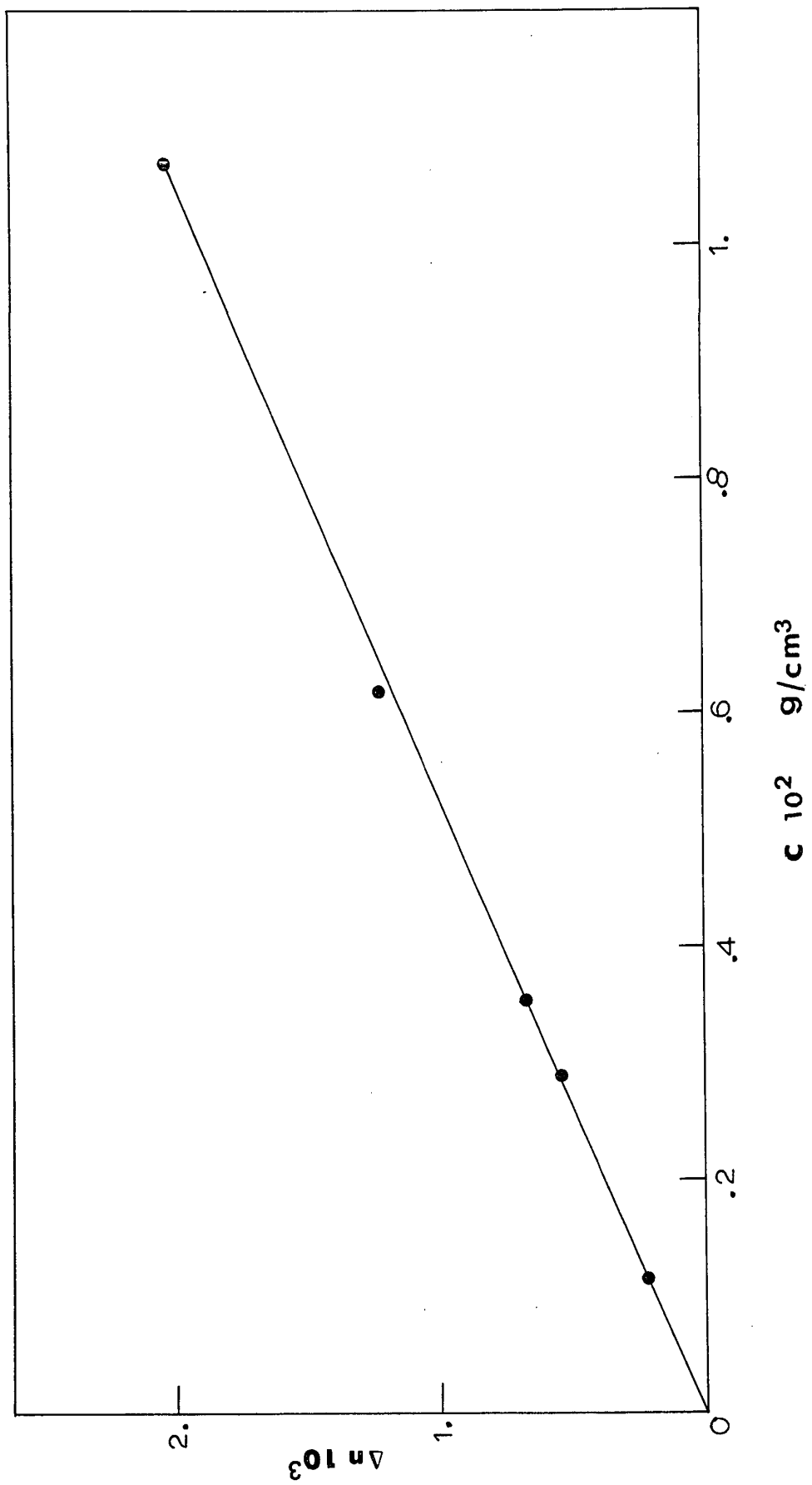
2.1.2.6 Determination of Refractive Index Increments

Schulz and Lechner note the inconvenience of determining (dn/dc) for a system under pressure. In the case of the PIB + 2-methylbutane system, light scattering measurements were made at temperatures considerably above the normal boiling point; dn/dc measurements with conventional instruments would also be inconvenient in this temperature range. Two procedures for obtaining dn/dc were used.

1. An experimental value of dn/dc was obtained at 5461 Å for the system at a single temperature and at atmospheric pressure. For PS + 2-butanone, dn/dc is well known²⁶. For PIB + 2-methylbutane, a value of 25° was measured using a Rayleigh differential refractometer. It is seen in Figure 2 that dn/dc is constant in the concentration range of the light scattering experiments, and equal to 0.188 cm³/g. Next the values of M_w for the PIB and PS fractions were measured by light scattering, giving the values listed in the materials

FIGURE 2

THE REFRACTIVE INDEX DIFFERENCE AS A FUNCTION OF
CONCENTRATION FOR PIB+2-METHYLBUTANE AT 24°



section. These values of M_w were taken to be independent of P and T, i.e. the macromolecules are assumed not to aggregate. Thus, at each value of P and T, a light scattering determination of the intercept $(c/l)_{\theta=0}$ allows a value of dn/dc to be calculated from the known value of M_w .

2. A number of expressions²⁹ relate the refractive index of a liquid to its density. The variation of density with P and T may be calculated using the recent, and accurate, Flory equation of state¹¹ for a polymeric³⁰ or a small-molecule liquid. Thus, using for instance the Lorentz-Lorenz expression, the variation of n_1 and n_2 may be found. The simple relation

$$\frac{dn}{dc} = \frac{n_2 - n_1}{\rho_2} \quad (24)$$

has been found²⁷ to give a reasonable approximation for dn/dc as a function of temperature for PIB + butyl ether. For the PS + 2-butanone system, the interpolated value of dn/dc ³¹ equal to $0.217 \text{ cm}^3/\text{g}$ at 22° and atmospheric pressure, was used to calculate n_2 for the polymer in the liquid state at 22° . Thus, values of dn/dc for other pressures could be calculated with eq. (24). For PIB + 2-methylbutane, the same procedure was followed using our own experimental dn/dc value of $0.188 \text{ cm}^3/\text{g}$. The values of dn/dc found in this way were in reasonable agreement with those calculated with the first method which assumed M_w to be constant. The largest difference was 6%.

Values of A_2 were calculated from the light scattering data, using values of dn/dc obtained with the above two methods, and were found to agree to within experimental error. The points in Figure 3 were obtained with the second method for dn/dc . The values of the refractive index increments are listed in Tables 1 and 2.

TABLE 1
REFRACTIVE INDEX INCREMENTS FOR
PIB+2-METHYLBUTANE

T°	P (bar)	0	30	60	90	110
24		0.188	0.186	0.184	0.183	0.181
57		0.204	0.201	0.198	0.195	0.194
64		0.207	0.204	0.201	0.199	0.197

TABLE 2
REFRACTIVE INDEX INCREMENTS FOR
PS+2-BUTANONE AT 22°

P (bar)	0	40	80	110
	0.217	0.217	0.216	0.215

2.1.2.7 Source of Errors and Accuracy

Light scattering is a fairly sophisticated method and requires much care for obtaining reliable data. The main sources of errors are:

- dust in the solutions, easily detected with the SOFICA instrument. However, quite a few experiments were not carried through because dust was detected in the solution.
- accurate values of the refractive index increments are needed. This is truly one of the severest limitations of the accuracy in this method.
- the extrapolations introduce errors if the measurements are not carried out at sufficiently low angles and concentrations in the case of non-linearity of the plots.

The values of dn/dc were reproducible within 2%. The accuracy is believed to be of the same order. M_w determinations are estimated to be accurate to $\pm 10\%$ ^{27,32}. In the case of PIB, the molecular weight was determined independently with heptane and found $M_w = 1.16 \times 10^6$, which compares well with the value given in section 2.1.2.1.

The second virial coefficient, A_2 , and the radius of gyration, $\langle S^2 \rangle^{1/2}$, are believed to be accurate within 20%, at low pressures and temperatures, as shown in Figures 3 and 4.

2.1.2.7 Source of Errors and Accuracy

Light scattering is a fairly sophisticated method and requires much care for obtaining reliable data. The main sources of errors are:

- dust in the solutions, easily detected with the SOFICA instrument. However, quite a few experiments were not carried through because dust was detected in the solution.
- accurate values of the refractive index increments are needed. This is truly one of the severest limitations of the accuracy in this method.
- the extrapolations introduce errors if the measurements are not carried out at sufficiently low angles and concentrations in the case of non-linearity of the plots.

The values of dn/dc were reproducible within 2%. The accuracy is believed to be of the same order. M_w determinations are estimated to be accurate to $\pm 10\%$ ^{27,32}. In the case of PIB, the molecular weight was determined independently with heptane and found $M_w = 1.16 \times 10^6$, which compares well with the value given in section 2.1.2.1.

The second virial coefficient, A_2 , and the radius of gyration, $\langle S^2 \rangle^{1/2}$, are believed to be accurate within 20%, at low pressures and temperatures, as shown in Figures 3 and 4.

FIGURE 3

THE SECOND VIRIAL COEFFICIENT, A_2 , AS A FUNCTION
OF PRESSURE FOR POLYISOBUTYLENE+2-
METHYLBUTANE AT: 24° , \blacktriangle ; 57° , \blacksquare ; 64° , \blacktriangledown .
AND FOR POLYSTYRENE+2-BUTANONE AT 22° \bullet .

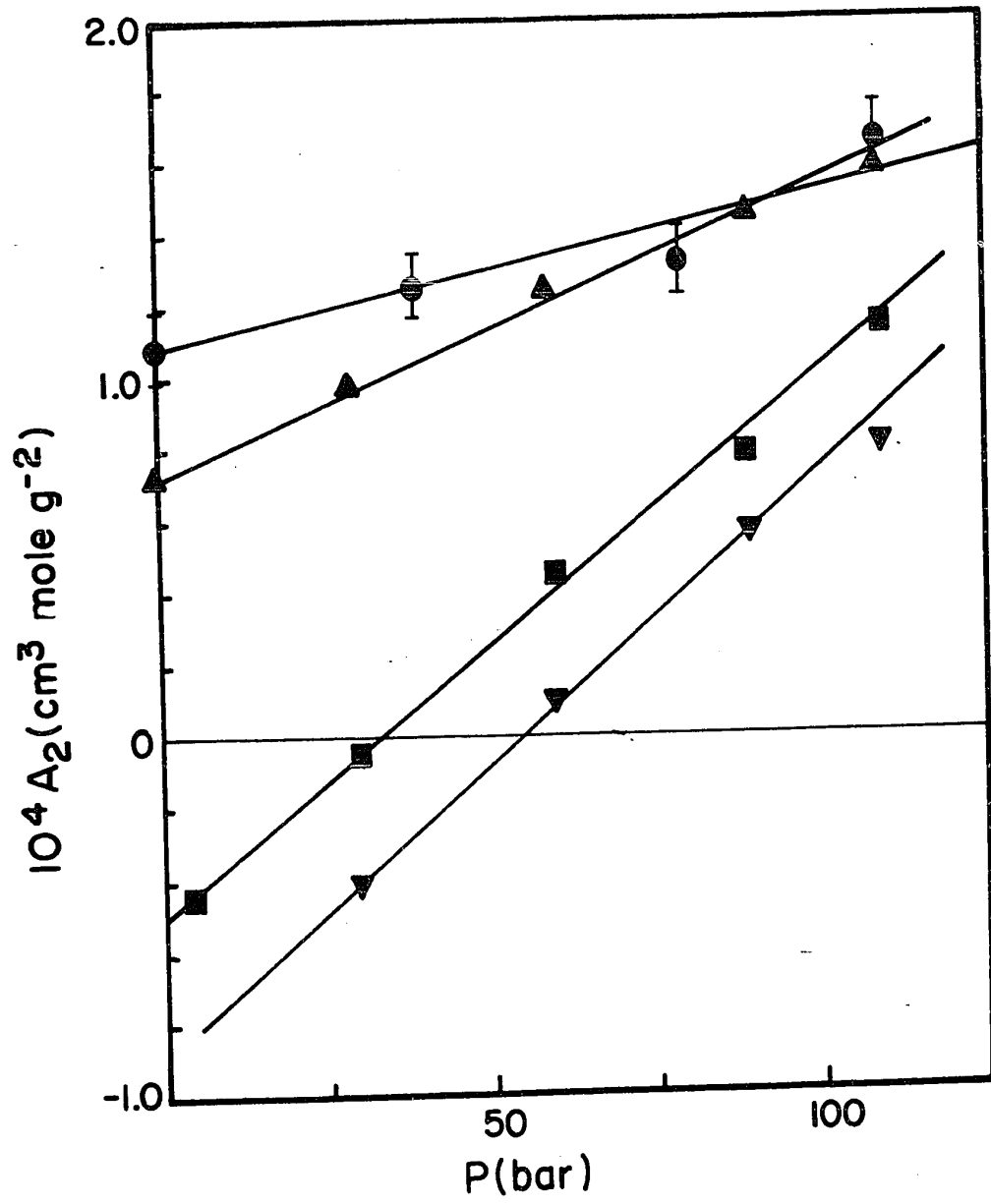
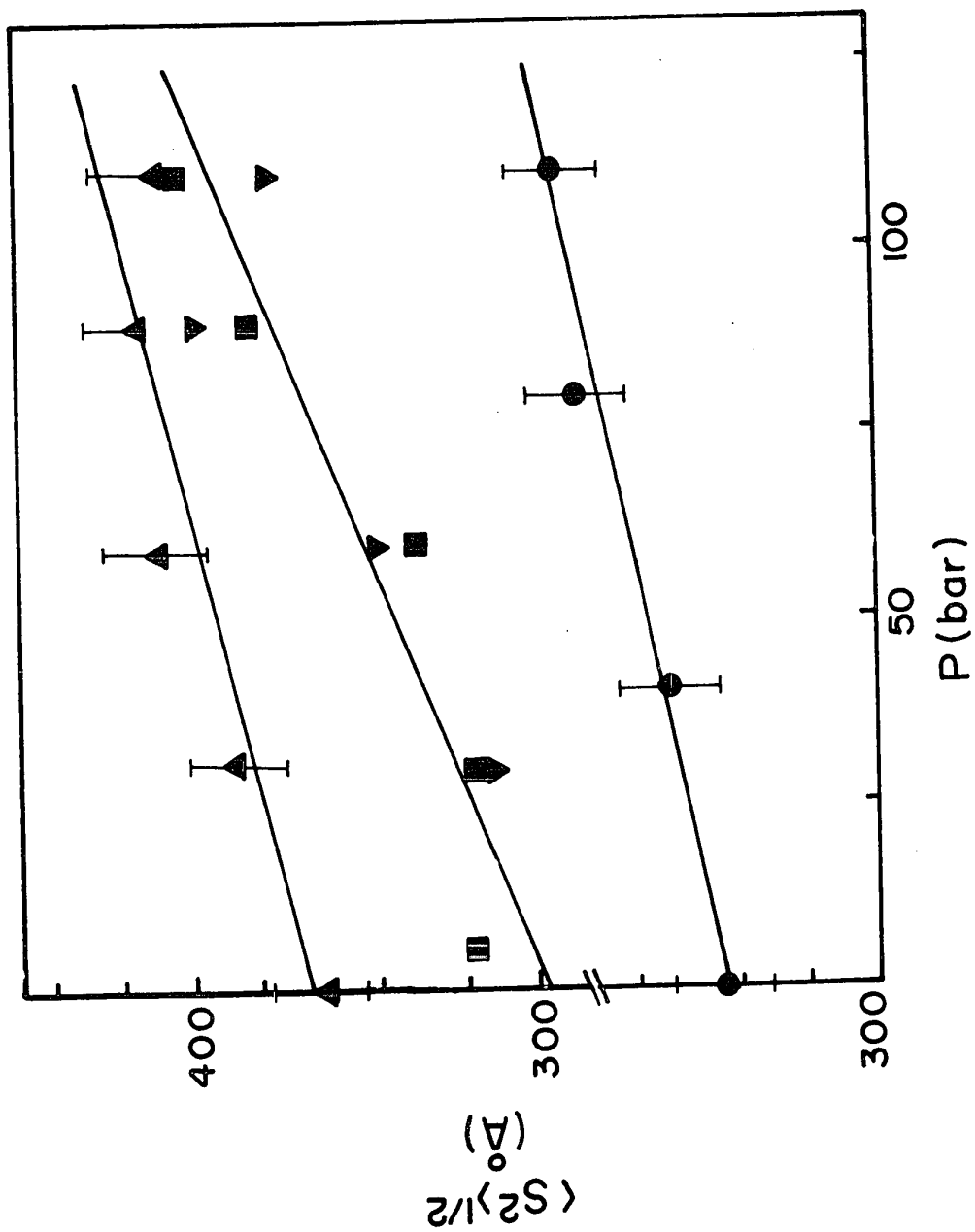


FIGURE 4
THE RADIUS OF GYRATION, $\langle S^2 \rangle^{\frac{1}{2}}$, AS A FUNCTION OF
PRESSURE FOR POLYISOBUTYLENE+2-METHYLBUTANE AT:
24°, ▲; 57°, ■; 64°, ▼;
AND FOR POLYSTYRENE+2-BUTANONE AT 22°, ●.



2.1.3 Results and Discussion

Figures 3 and 4 show the values of A_2 and $\langle S^2 \rangle^{1/2}$ as a function of pressure for PIB+2-methylbutane at 24, 57 and 64°, and for PS+2-butanone at 22°. The heat of dilution of the PS+2-butanone system is found by calorimetry to be exothermic, but very small; A_2 and $\langle S^2 \rangle^{1/2}$ should therefore be almost independent of temperature for this system and the light scattering measurements were confined to the one temperature. Both A_2 and $\langle S^2 \rangle^{1/2}$ increase with pressure for both systems in accord with negative values of ΔV_M .

The Berry $(c/l)^{1/2}$ plot was used for two extreme values of the pressure in the case of the PS+2-butanone system and the PIB + 2-methylbutane system at 24°. In the former case the values of M_w , A_2 and $\langle S^2 \rangle^{1/2}$ were, respectively, decreased by 3%, increased by 4% and decreased by 5%. In the latter case, the corresponding changes were a decrease of 1%, a decrease of 2% and an increase of 6%. These changes were ignored, however, since they are within the experimental error.

2.1.3.1 LCST Values in the PIB+2-Methylbutane System

Values of the LCST have been obtained¹³ for different molecular weights of PIB in 2-methylbutane at the saturated vapour pressure. Extrapolation to infinite mol. wt. gives a θ -temperature, associated with the LCST, of 45°. This is consistent with the present results where A_2 is positive at 24°

and zero pressure, but decreases to negative values at 57° and 64°. Assuming $(\partial A_2/\partial T)_P$ to be constant through this temperature range, one finds that, under zero pressure conditions, $A_2 = 0$ at $\theta = 43^\circ$. This value of the θ -temperature is in good agreement with that found from the LCST measurements. Studies have been made of the effect of pressure on the LCST of PIB+2-methylbutane, i.e. of the (P,T) projection of the critical line. For a fraction of PIB which gives an LCST at 50° under zero pressure, one has^{13b} $(dT/dP)_C = 0.44$ deg/bar. From the thermodynamic analysis³³ of critical solution points we have

$$\begin{aligned} (dT/dP)_C &= T(\partial^2 V/\partial x_2^2)_C / (\partial^2 H/\partial x_2^2)_C \\ &= T(\partial \Delta \bar{V}_1/\partial x_2)_C / (\partial \Delta \bar{H}_1/\partial x_2)_C \end{aligned} \quad (25)$$

Neglecting β_1 and α_1 in eqs. (7) and (8), eq. (25) becomes

$$(dT/dP)_C = -(\partial A_2/\partial P)_T / (\partial A_2/\partial T)_P \quad (26)$$

The values of the LCST as a function of pressure thus correspond to a constant value of A_2 . For a polymer of infinite mol. wt., $A_2 = 0$ along the critical line, and all points along this line correspond to θ -temperatures, unperturbed polymer dimensions and Gaussian distribution of segments. Values of A_2 at 24° and 64° at $P = 0$ gave $(\partial A_2/\partial T)_P$ at the mean temperature of 44°. This value and a corresponding mean value of

$(\partial A_2/\partial P)_T$ were used in eq. (19) which gives $(dT/dP)_c = 0.3$ deg/bar in reasonable agreement with the value of 0.44 deg/atm obtained from the pressure dependence of the LCST.

It is of interest to compare the results obtained by light scattering²² with direct measurements¹³ for PIB+pentane. Wolf's results²² extrapolate to an LCST equal to 70° at zero pressure, the slope of the critical line, dT/dP being equal to 0.13 deg/atm. Patterson et al.^{13b} find 80° and 0.42 deg/atm respectively. The agreement is good for the LCST, but only qualitative for the critical slope.

2.1.3.2 Relative Partial Molar Volumes and Heats of the Solvent

The Krigbaum-Carpenter-Kaneko-Roig (KCKR) theory³⁴ was used to obtain the $h(z)$ function in order to furnish values of A_2^{conc} for use in eqs. (18) and (19). In this theory, values of the ρ parameter equal to 0, 0.2 and 1 give results corresponding to, respectively, the Casassa-Markovitz³⁵, Kurata-Fukatsu-Sotobayashi-Yamakawa³⁶ and the Flory-Krigbaum³⁷ theories. We used an intermediate value of 0.4 which was originally favoured³⁴ on the basis of a comparison with experiment. The following values²³ of the parameter A were used in conjunction: PIB, 740×10^{-11} ; PS, 670×10^{-11} . The $h(z)$ function given by the KCKR theory then allowed A_2^{conc} to be calculated from values of A_2 obtained in the dilute concentration range. Its pressure dependence was used in eq. (18) to yield

the following values of k_V for the PIB+2-methylbutane system: 24° , -3.5×10^{-2} ; 57° , -4.6×10^{-2} and 64° , -4.5×10^{-2} .

Direct measurements of ΔV_M have not, to our knowledge, been reported. However, comparison can be made with ΔV_M values³⁸ for PIB with the isomer, n-pentane at 25° . The values are symmetrical in volume fraction, with $k_V = -5.0 \times 10^{-2}$. For the PS+2-butanone system, we find $k_V = -3.6 \times 10^{-2}$. Values of $\Delta V_M/V$ have been obtained by Flory and collaborators¹¹, whose results are consistent with a value of $k_V = -3.3 \times 10^{-2}$.

From the change of A_2 at zero pressure between 24° and 57° we calculate a value of the enthalpic parameter $\chi_H = -0.12$ with $\rho = 0.4$ in the KCKR theory. Experimental heats of dilution are not available for this system. However, heats of mixing PIB with 2-methylbutane to great dilution of the polymer have been measured, and are very similar to those measured for PIB in n-pentane, where heats of dilution are available³⁹. The quantity χ_H defined by eq. (17) is found to be independent of concentration for PIB+n-pentane. In terms of the volume fractions, $\chi_H = -0.14$. It seems that fairly accurate values of the volumes and heats of dilution may be obtained from the light scattering measurements.

2.1.3.3 Comparison of the Pressure Dependence of A_2 with Predictions of Newer Theories

The second virial coefficient, A_2 , is related to the polymer-solvent interaction parameter, χ , through eqs. (9) and

(10). The following equation has been used to predict the pressure and temperature dependence of χ at low concentration of polymer, but still in the "concentrated" range, i.e. assuming interpenetration of the macromolecules:

$$\chi(P,T) = c_1 \left[-\frac{\tilde{U}_1}{\tilde{T}_1} \nu^2 + \frac{1}{2} \tilde{C}_{p,1}(P_1, T_1) \left[\tau + \frac{\tilde{P}_1 \tilde{V}_1^2}{\tilde{P}_1 \tilde{V}_1^2 + 1} \pi \right]^2 \right] \quad (27)$$

The quantities \tilde{U}_1 and $\tilde{C}_{p,1}$ are the reduced configurational energy and heat capacity of the pure solvent. The Flory theory¹¹ essentially predicts these quantities, using a van der Waals model of the liquid state and a partition function similar to the Hirschfelder-Eyring cell partition function. Then \tilde{U}_1 , $\tilde{C}_{p,1}$ and \tilde{T}_1 are given in terms of the reduced quantities \tilde{P}_1 and \tilde{V}_1 of the solvent. The τ parameter is a measure of the difference in degrees of thermal expansions or free volumes of the two components:

$$\tau = 1 - T_1^*/T_2^* \quad (28)$$

The temperature reduction parameters T^* may be obtained from the equation of state quantities of the pure components following, for instance, the prescription of Flory and collaborators. The equation of state data for PS+2-butanone are listed in Table 7, with c , taken equal to 1.0, and T^* equal

to 4557 K and 7420 K for 2-butanone and PS respectively.

The data of PIB+2-methylbutane are given in Table 3.

TABLE 3

EQUATION OF STATE PARAMETERS FOR PIB+2-METHYLBUTANE

Component	T^* (K)	P^* (cal/cm ³)	v_{sp} (cm ³ /g)	c_1
(2) PIB ^{13b}	7580	107.	0.95	
(1) 2-methyl- butane ^{13b}	4098	100.5	1.19	1.06

The γ^2 parameter expresses the difference of chemical nature of the components which results in a weakness of the energy of the (1-2) contacts relative to the (1-1) and (2-2) contacts. The π parameter expresses a difference in P^* reduction parameters similar to eq. (28): $\pi = P_1^*/P_2^* - 1$, and the parameter $3c_1$ is the number of external, volume-dependent degrees of freedom of the solvent molecule. At zero pressure, eq. (27) becomes the Flory theory expression for χ (eqs. 49-51 of ref. 14a), except that the Flory parameter s_2/s_1 is set equal to unity, and only second powers of the quantities τ and γ are retained. In treating the thermodynamics of the PIB+n-pentane system at 25^o, Eichinger and Flory^{14d} fit their theory to heats of solution in order to evaluate the $\gamma^2 = X_{12}/P_1^*$ parameter, and then predict χ (at zero pressure). At low polymer concentration the predicted $\chi = 0.65$ which would

erroneously give large negative values of A_2 . We have decided to fit both the γ^2 and τ parameters with the zero-pressure data for A_2 , and then use the theory to predict the pressure dependence of A_2 . Thus, for the PIB+2-methylbutane system at zero pressure we take $A_2 = 0$ at $\theta = 44^\circ$, where $\chi_H = -T(\partial\chi/\partial T)_P = -0.12$ calculated for the "concentrated" solution as described in the preceding section. The fitted γ^2 parameter is small as expected from the close chemical similarity of the polymer and solvent; it corresponds to a value of $\chi_{12} = 1.8 \text{ cal/cm}^3$. The fitted τ parameter, equal to 0.34, was 30% smaller than the value calculated from the T^* parameters obtained from equation of state data. The predicted A_2 increases with pressure, the curve being slightly concave downward. In the 0-100 bar range however, it is virtually a straight line. The slopes are 24° : 2.2×10^{-6} and 57° : $3.4 \times 10^{-6} \text{ cm}^3 \text{ mole g}^{-2} \text{ bar}^{-1}$. This is in fair agreement with the values of $(\partial A^{\text{conc}}/\partial P) = 1.7 \times 10^{-6}$ and $2.1 \times 10^{-6} \text{ cm}^3 \text{ mole g}^{-2} \text{ bar}^{-1}$ found experimentally for the PIB+2-methylbutane system (using the KCKR excluded volume theory with $\rho = 0.4$ to give $h(z)$).

An analogous calculation was performed for the polystyrene+2-butanone system. Values of γ^2 and τ were obtained by fitting eq. (27) to the value of $A_2^{\text{conc}} = 1.9 \times 10^{-4} \text{ cm}^3 \text{ mole g}^{-2}$ at 22° and zero pressure. Calorimetric measurements*

* cf. section 3.1

small and we took $\chi_H = 0$ at 22° . The value of the fitted γ^2 parameter was small corresponding to $\chi_{12} = 1.8 \text{ cal/cm}^3$, while τ was approximately equal to the value calculated from equation of state data, and found to be 0.34. The predicted pressure dependence of A_2 at 22° is $0.9 \times 10^{-6} \text{ cm}^3 \text{ mole g}^{-2} \text{ bar}^{-1}$, which is again in fair agreement with the experimental value of $\partial A_2^{\text{conc}} / \partial P = 1.3 \times 10^{-6} \text{ cm}^3 \text{ mole g}^{-2} \text{ bar}^{-1}$. We conclude that the theoretical eq. (27) gives reasonable, if not quantitative, agreement with experiment.

2.1.3.4 Pressure and Temperature Dependence of the Radius of Gyration

Values of $\langle S^2 \rangle^{1/2}$ for the PIB molecules in 2-methylbutane at different T and P were plotted against the corresponding values of A_2 . A single curve was obtained showing that the effect of pressure on the chain dimensions is similar to that of temperature. Both act through the polymer-solvent interaction parameters B and z, which also bring about the change of A_2 . The radius of gyration,

$$\langle S^2 \rangle^{1/2} = \langle S_0^2 \rangle^{1/2} \alpha(z) \quad (29)$$

is the same whether the expansion coefficient, $\alpha(z)$, is changed through P or T. On the other hand, the results of Schulz and Lechner¹⁹ (in their Table 4) for PS in trans-decalin and toluene do not give a single curve of the radius of gyration at different P and T against A_2 . For the same A_2 , $\langle S^2 \rangle^{1/2}$

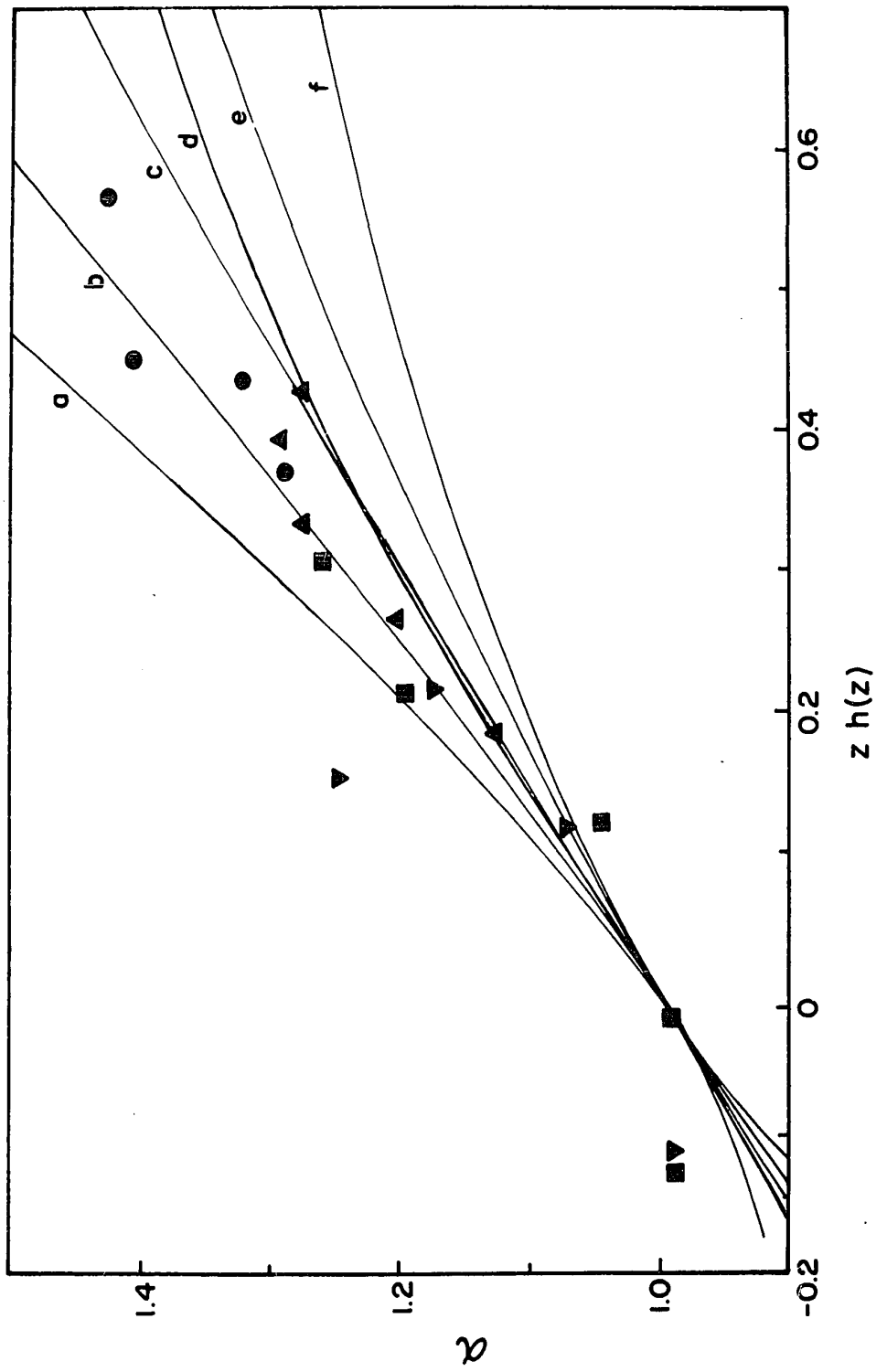
values are lower when obtained at higher pressures, indicating that the unperturbed dimension $\langle S^2 \rangle^{1/2}$ is a decreasing function of pressure, as noted¹⁹. This result may indicate an effect of the solvent packing on the population of conformations or rotational isomers of the polystyrene. It is usually believed that the solvent has little effect on the unperturbed dimensions of the macromolecule, but the possibility⁴¹ should not be disregarded. Even a small effect of solvent packing on the rotational isomer equilibrium would have important consequences in polymer solution thermodynamics.

Values of $\alpha(z)$ were obtained from $\langle S^2 \rangle^{1/2}$ with a value of $\langle S_0^2 \rangle^{1/2}$ of PIB equal to 320 \AA , read off the $\langle S^2 \rangle^{1/2}$ versus A_2 plot at $A_2 = 0$. For PS+2-butanone, an approximate value of $\langle S_0^2 \rangle^{1/2} = 260 \text{ \AA}$ was obtained by extrapolation and $\alpha(z)$ was determined. Using eq. (9) and the values of A given in the preceding section, values of $zh(z)$ were computed from A_2 for both systems. Figure 5 shows $\alpha(z)$ against $zh(z)$, where it may be seen that the points for both systems and for the different T and P do approximately fall on a single curve, as expected from theory. This result does not change on considering the effects of polydispersity on the values of $\langle S^2 \rangle^{1/2}$ and A_2 (see below).

A number of similar closed expressions²³ relate the expansion factor α of the polymer coil to z , i.e. they give the ordinate in Figure 5. We have used the Fixman-Stockmayer expression,

FIGURE 5

The coil expansion factor, α , for the polymer-solvent systems at various pressures and temperatures (symbols as in Figures 1 and 2). The abscissa, $zh(z)$, is proportional to A_2 as in eq. (9). Theoretical curves a, b, c are given by the Fixman-Stockmayer expression for $\alpha(z)$, eq. (30) and the Krigbaum-Carpenter-Kaneko-Roig theory for A_2 with ρ equal to respectively 0 (Casassa-Markovitz), 0.4 and 1 (Flory-Krigbaum). Theoretical curves d, e, f are given by the Stockmayer modification of the Fox-Flory expression, eq. (31) and the KCKR theory with ρ equal to respectively 0, 0.4 and 1.



$$\alpha^3 - 1 = 2z \quad (30)$$

and the Stockmayer modification of the Flory-Fox relation:

$$\alpha^5 - \alpha^3 = (134/105)z \quad (31)$$

The abscissa of Figure 5, $z(hz)$, was obtained through the KCKR theory with the three values of the ρ parameter: 0, 0.4 and 1. Figure 5 shows the resulting six curves of $\alpha(z)$ against $zh(z)$. We note that the $zh(z)$ function is the same as $\psi_{\alpha_s}^3$ used in some other treatments⁴².

The PIB+2-methylbutane data are consistent with either of the two $\alpha(z)$ formulae. However, the difference in predictions for $\alpha(z)$ becomes more marked at large z and the PS+2-butanone data are in better agreement with the Fixman-Stockmayer than with the modified Flory-Fox prescription.

We have also calculated α against $zh(z) \equiv \psi_{\alpha_s}^3$ for three other combinations of theories for A_2 and α . These were as given by eqs. (17) to (22) of ref. 42, and corresponded to the original Flory-Krigbaum-Orfino A_2 expression combined with the original Flory α expression, the combination of the modified expressions, and the Kurata-Fukatsu-Sotobayashi-Yamakawa A_2 combined with the Yamakawa-Tanaka α expressions. The first and third recipes gave curves of α against $zh(z)$ close to curves (c) and (d) in Figure 5 while the second gave a lower curve towards (e). The experimental points lie

slightly above these three curves, but the difference is probably within experimental error.

2.1.3.5 Effects of Polydispersity

We have used the Yamakawa-Kurata treatment⁴³ to assess the effect of polydispersity on the value of A_2 . Their series expansion for $h(z)$ is:

$$h(z) = 1 - 2.865 Q'_w z_w \dots \quad (32)$$

Here z_w is the value of z corresponding to the weight-average molecular weight of the sample, Q'_w is a parameter greater than unity in the case of polydispersity. For the present polydisperse PIB sample, characterized by $h \sim 2.2$, Figure 1 of ref. 43 indicates that $Q'_w \sim 1.07$. Following eq. (32) we have replaced z in the closed expressions for $h(z)$ the product $Q'_w z_w$. We find that a monodisperse fraction of the same M_w would have values of A_2 approximately 4% higher than those found experimentally with our polydisperse sample. The treatment of Cassassa⁴⁴ also indicates that the change in A_2 would be very small, and it seems reasonable to ignore it.

In the case of the coil expansion factor α , Kurata and Stockmayer²³ give the series expansion

$$\alpha^2 - 1 = (134/105) q_s z_w + \dots \quad (33)$$

where the factor introduced by polydispersity, $q_s = 1.257$ for $h = 2.2$. Following ref. 23, we have assumed that the product $q_s z_w$ may be used in the closed expressions, i.e. eqs. (30) and (31), in order to correct the values for α for the polydispersity of the PIB sample. We find that the difference between the value of α and unity is decreased by approximately 15%. The points in Figure 5 for the PIB+2-methylbutane system would be lowered and fall closer to the curve c than to b. It seems, however, that the general conclusions of the last section would remain, particularly since the points in Figure 5 for the polystyrene+2-butanone system would be virtually unchanged, corresponding to the very low polydispersity of the this polymer sample.

2.2 EFFECT OF PRESSURE ON PHASE BOUNDARIES

Every high polymer-solvent mixture shows an LCST (no matter how close to the critical point of the solvent), because the difference in free volume between the two components provides a large enough contribution to χ (see for instance eq. 27) to bring it up to the critical value and thus making phase separation to occur. However, at lower temperatures, this solution may or may not undergo phase separation. Here it is the difference of intermolecular forces between the polymer and the solvent (the chemical difference), represented by the term in γ^2 of eq. (27), which

FIGURE 6
ZIMM PLOT FOR PS+2-BUTANONE AT 22° AND
ATMOSPHERIC PRESSURE

c is the concentration expressed
in g/cm^3 , I is the excess scattered
light due to the polymer, and has
been corrected for the variations
of the scattering volume.

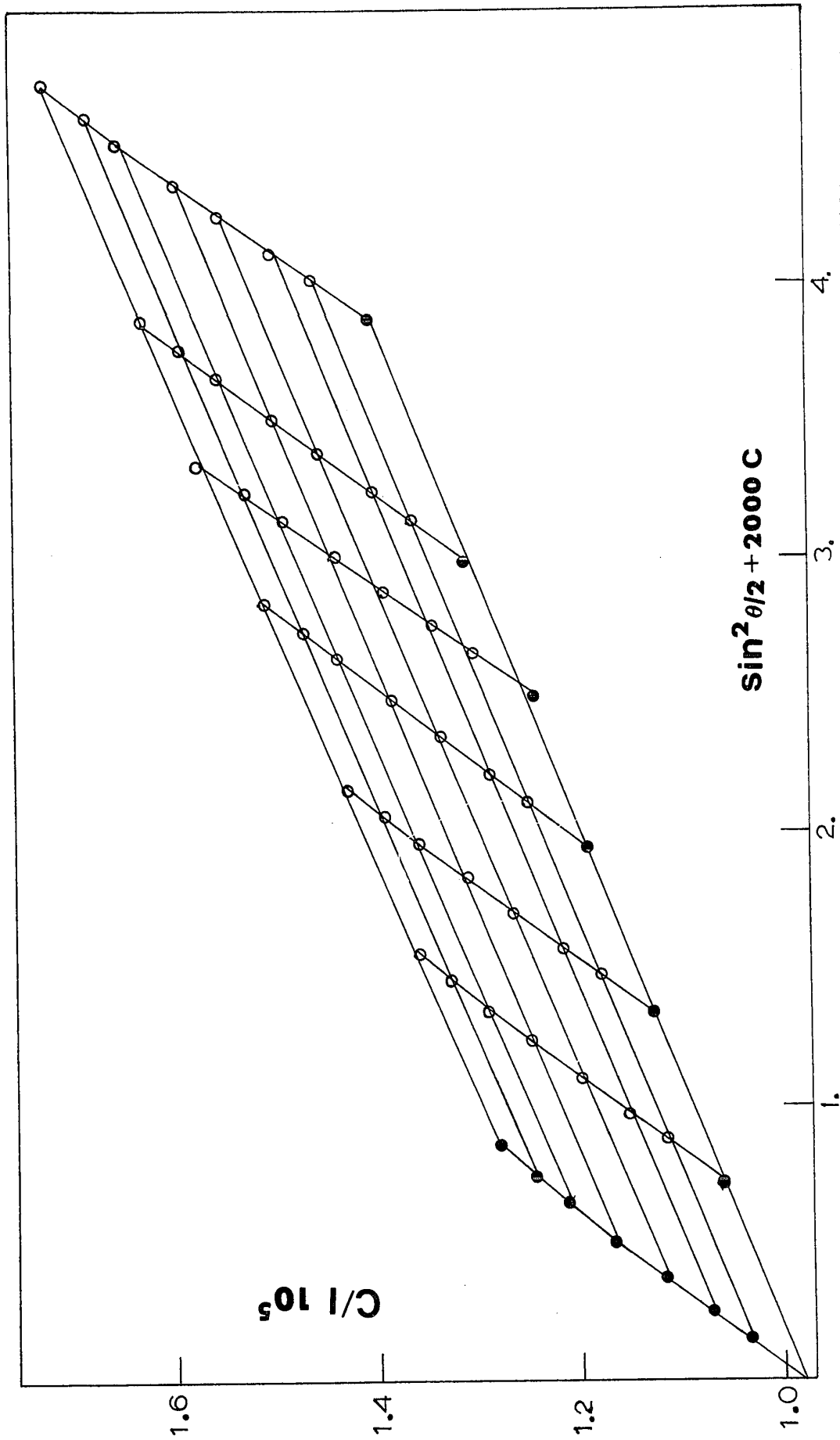
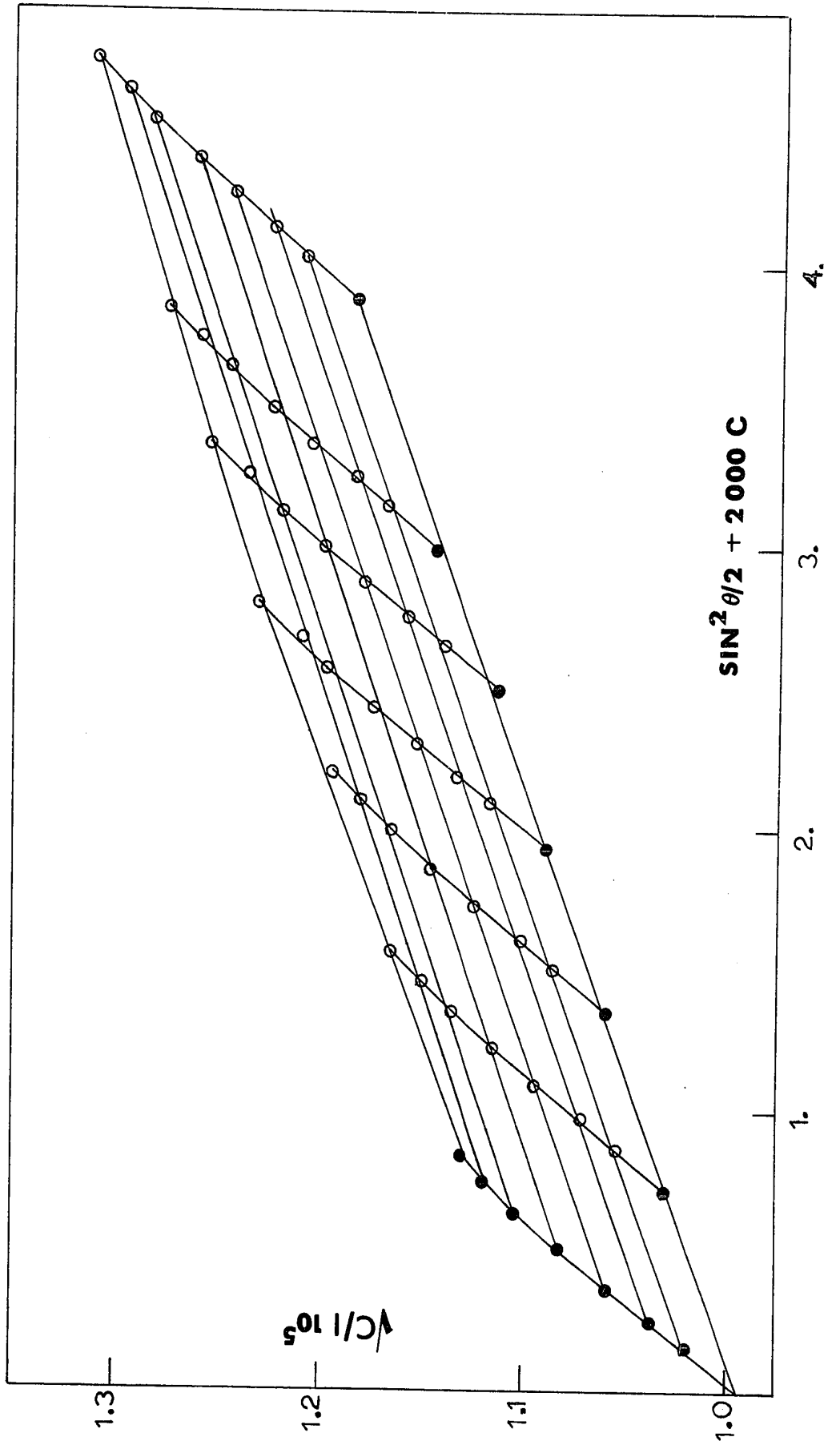


FIGURE 7
BERRY PLOT FOR PS+2-BUTANONE AT 22° AND
ATMOSPHERIC PRESSURE



counts most. Even more, this intermolecular forces dissimilarity can be large enough to render the components immiscible at equilibrium vapour pressure, at any temperature.

Our group has been active in the study of the pressure dependence of LCS Temperatures^{13b}. The magnitude of the critical line slope is typically about 2 bar/deg. at the LCST. In the vicinity of the UCST however, the free volume contribution is of less importance, and therefore, the pressure effect should be smaller. Experimentally⁴⁵ it was found that the UCST pressure dependence was smaller by a factor of 100 than the corresponding one at the LCST.

This work is a systematic, but only qualitative, investigation of the UCST pressure dependence. Three different type of polymer were studied: polystyrene (PS), polyisobutylene (PIB) and poly (dimethylsiloxane) (PDMS).

2.2.1 Experimental

2.2.1.1 Materials

Five PIB fractions were used of $M_v = 1,250, 30,000; 90,000; 400,000$ and $1,000,000$. Two Dow Corning PDMS samples were of $M_n = 22,000$ and $M_v = 203,000$. Of the six PS samples studied, five were purchased from Pressure Chemical Co. (Pittsburgh, Pa.). They were of 900; 2030; 4000; 10,000; 19,800 nominal molecular weight; the ratio M_w/M_n being

respectively 1.10, 1.10, 1.10, 1.06, 1.06. In addition a Monsanto PS sample, LUSTREX, of $M_v = 200,000$ was studied.

The cyclohexane, pentane, hexane, benzene and acetone were Fisher Certified reagents. Octane, dodecane, hexadecane and 2, 2-dimethylbutane were purchased from Aldrich Chemical Co. The 1,4-dioxane was a "Baker Analyzed" reagent, the isopropanol was an Anachemia product (99% pure). None of these solvents was further purified.

2.2.1.2 The Apparatus

A stainless steel cross, purchased from Aminco (Silver Spring, Md.), provided the optical cell. The two glass windows, of 13 mm diameter and 9 mm thick, were sealed with Teflon o-rings. The total volume of the cell was about 1.2 cm^3 including the volume of the tubing from the cell to the valve V4 as seen in Figure 1. The pressure circuit was filled with the solvent used for making the solution, as mentioned in section 2.1.2.5. The cell was heated by a heating tape and the temperature measured by a thermocouple, located in the body of the cell, approximately 1 mm away from the solution. Uniform temperature was ensured by the large metal block surrounding the small cavity accessible to the solution.

2.2.1.3 Procedure

A solution of known concentration was prepared and transferred with a syringe into the cell. The "cloud point" curve was generated by setting the temperature, awaiting temperature equilibrium for about 15 to 30 minutes and finally varying the pressure. Several readings were taken for each transition by raising and lowering the pressure. Then the temperature was raised, equilibrated, and the same procedure was repeated.

2.2.1.4 Source of Errors

The pressure system used has been described in section 2.1, and the pressure readings are accurate to 0.5 bar. The temperature determination was accurate within 0.3° . However, for some LCST determinations, the accuracy may be no better than 1° . The concentration was known approximately (the relative error is 5%) only, but accurately enough to allow comparison to be made. The P,T curve does not vary much^{13b} in the concentration range where we worked. The polydispersity of the polymer samples brings uncertainty to the determination of critical temperatures. The precision therefore is of the order of 1° , whereas the accuracy should be within 5° . Precision and accuracy for $(dp/dT)_c$, are believed to be of the same order, i.e. 10%.

2.2.2 Results and Discussion

PIB+BENZENE

The PIB+benzene system is attractive with a convenient Theta temperature of 25° . In addition the volume of mixing⁴⁶ is positive and large and should therefore lead to a fairly small dP/dT , along the critical line. However, there are some technical difficulties due to the small refractive index increment (for that reason, this system was not studied by light scattering). A 0.04 g/cm^3 solution was made with a fractionated PIB sample of $M_V = 400,000$. Transitions were measured up to 300 bars in the temperature range of 16 to 28° . The critical line is straight and has a slope equal to 21 bar/deg. The extrapolated UCST at zero pressure is 15° .

PIB+DIOXANE

The UCST and LCST were first measured in sealed tubes using the usual set-up described elsewhere⁴⁷. A 0.01 g/cm^3 solution with a PIB sample of $M_V = 30,000$ gave a UCST equal to 111° and an LCST equal to 304° ; a molecular weight of 90,000 yields respectively 126° and 291° for the UCST and LCST.

The pressure dependence of the UCST for this system was studied on three different molecular weight samples, the concentration being in the range of 0.02 to 0.03 g/cm^3 . The 1,250 number molecular weight sample (Napvis 30) gave dP/dT ,

along the critical line, equal to 30 bar/deg; the 30,000 molecular weight PIB (the sample used in sealed tubes) gave 33 bar/deg, which is not significantly different from the value of the previous sample. A PIB fraction of $M_w = 10^6$ gave a slightly lower value, equal to 25 bar/deg. A more concentrated solution, 0.1 g/cm^3 gave exactly the same slope.

PIB+ACETONE

No dissolution occurs at the vapour pressure of the solvent for high molecular weight PIB samples. The Napvis 30 sample (molecular weight of 1,250) gave a UCST pressure dependence equal to 55 bar/deg at 52° , the extrapolated UCST; the LCST is located at 191° at zero pressure, $(dP/dT)_c$ being equal to 1.3 bar/deg.

For these three PIB systems, the UCST increases with pressure. The volume of mixing is accordingly positive.

PDMS+ISOPROPANOL

A Dow Corning sample of molecular weight 22,000 was investigated. The UCST, at the vapour pressure of the solvent is 43° . The slope of the critical line, dP/dT , is found equal to 45 bar/deg.

PDMS+ACETONE

Another Dow Corning PDMS, of $M_v = 203,000$, gave a UCST equal to 66° , at the vapour pressure of acetone. The value of $(dP/dT)_c$ was found equal to 75 bar/deg.

The concentrations, in both PDMS solutions, were 0.02 g/cm^3 . Again in the PDMS systems, as in the PIB solutions, the volume of mixing is positive.

PS+CYCLOHEXANE

The UCST pressure dependence for this system has been reported earlier⁴⁵, our value of 300 bar/deg for $(dP/dT)_c$ agrees very well with theirs. The UCST at the vapour pressure of the solvent is 22° . ΔG_M being almost insensitive to any pressure change, ΔV_M is very small for this particular molecular weight.

PS+NORMAL ALKANES

Normal alkanes are considered non-solvents for PS. Therefore, in order to achieve dissolution in a reasonable range of temperature and pressure, low molecular weight PS fractions were chosen. In addition one branched alkane, 2,2-dimethylbutane, was studied.

Values of the UCST at different pressures up to 300 bars are reported in Figure 8 for a PS of 2030 molecular weight with hexane, octane, dodecane, hexadecane and an isomer of hexane: 2,2-dimethylbutane. It is seen that an increase of the chain length of the alkane (from C_6 to C_{16}) raises the UCST and the value of the slope of the critical line, from -10 bar/deg for pentane to almost "infinity" with dodecane and hexadecane. In other words, the volume of mixing is negative when PS is mixed with pentane and large in magnitude, then increases in this series until a zero value is obtained with the higher alkane. It is quite clear that the volume of mixing should be more negative for pentane than for hexadecane: the difference in free volume between PS+pentane and PS+hexadecane (represented by the differences in thermal expansivities) is larger for the former system, providing thus a larger negative contribution to ΔV_M .

It is of interest to study the critical line for one solvent with various PS molecular weights. The results are given in Table 4 for three solvents. The general picture is that for a given solvent, increasing molecular weights bring about a decrease in $\left| \left(\frac{dP}{dT} \right)_c \right|$ values. The explanation can be visualized by using different critical lines in the P, T plane, corresponding to the different molecular weights, as shown in Figure 9 (reproduced from Figure 7 of reference 21). Curve (a) would correspond to a low molecular weight PS, soluble at

FIGURE 8

(P,T) CLOUD POINT CURVES FOR A POLYSTYRENE
FRACTION OF MOLECULAR WEIGHT 2030 IN ALKANES

- HEXANE
- OCTANE
- DODECANE
- △ HEXADECANE
- ▽ 2,2-DIMETHYLBUTANE

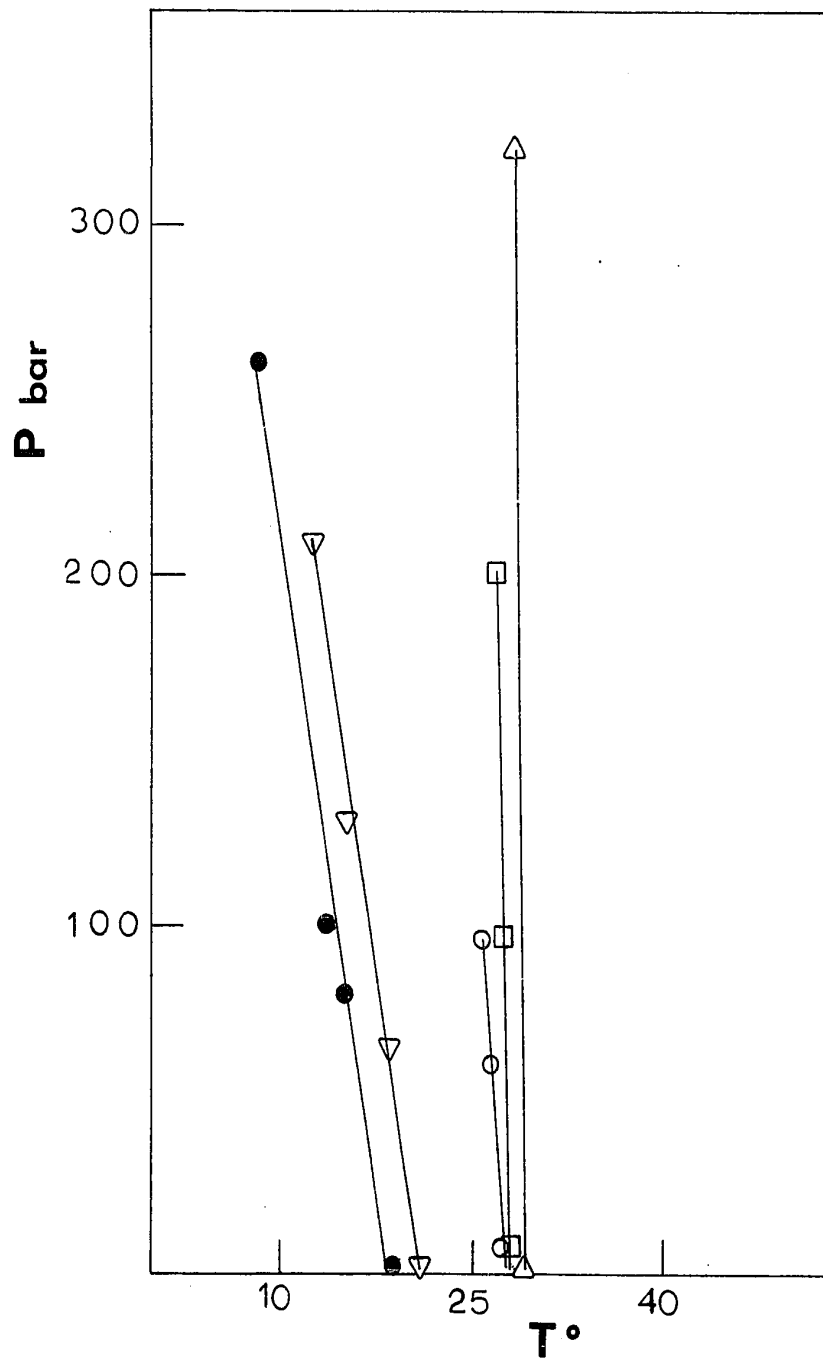
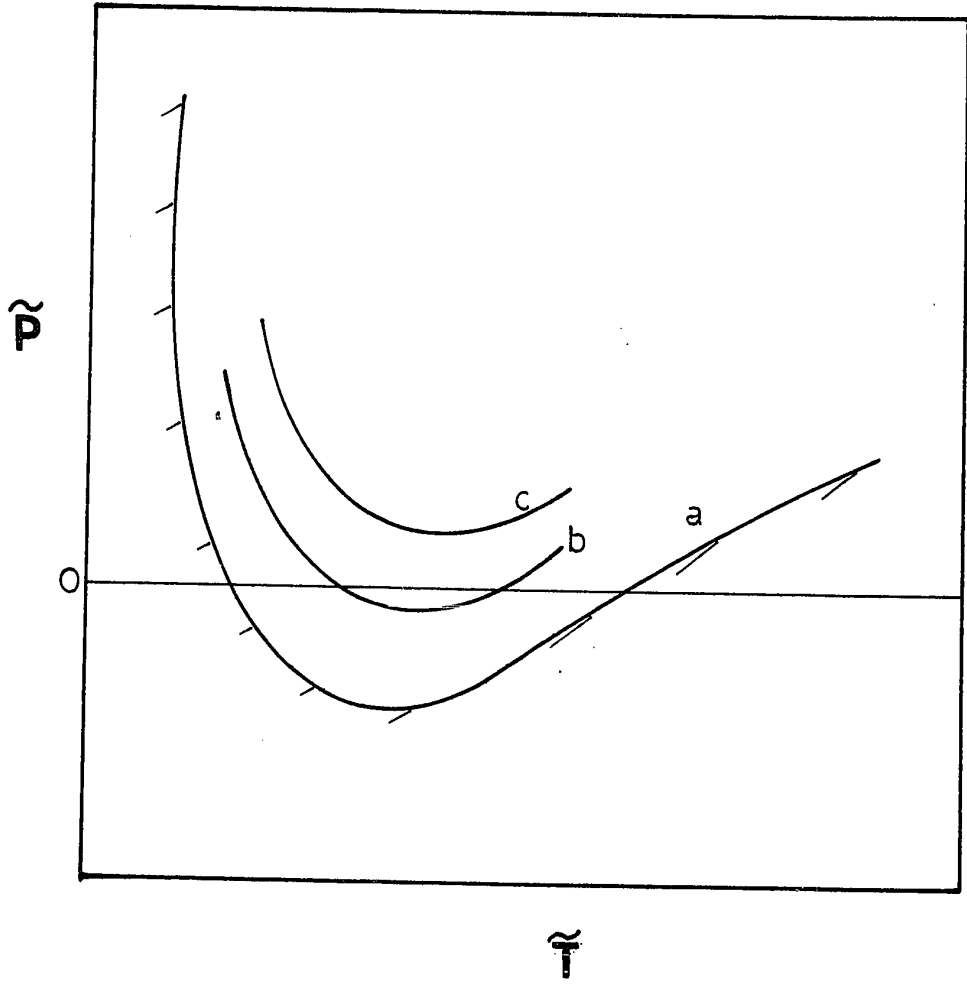


FIGURE 9

CRITICAL LINES IN REDUCED PRESSURE AND
TEMPERATURE COORDINATES

The three critical lines a, b, c correspond to decreasing critical χ values as obtained in the case of increasing polymer chain length.



the vapor pressure of the solvent, presenting a UCST and an LCST. A higher molecular weight sample brings the critical line up to curve (b) which already shows a flatter slope $(dP/dT)_c$ at the UCST than curve (a), and the UCST and LCST are closer now. Curve (c) would be obtained by an even higher PS molecular weight which is not soluble at any temperature under the vapour pressure of the solvent. In other words, going from curve (a) to (b) and to (c) is brought about by decreasing the critical value of χ .

This PS series does not include any system behaving according to curve (c) of Figure 9; however, the required hypothetical PS molecular weight can be estimated from Figure 10. This is the well known Shultz-Flory plot, showing $1/T_c$ versus $(1/r^{1/2} + 1/2r)$. A straight line is expected⁴⁸, cutting across the ordinate at the Theta temperature θ , the slope being $(\psi_1\theta)^{-1}$, where ψ_1 is the Flory parameter which represents the entropy of dilution of the solution. The plot, however, is not composed of two straight lines, one for the UCST the other for the LCST. The curvature is due to a variation of ψ_1 , with temperature⁴⁹. The results show a positive entropy of dilution in the UCST region, a negative one in the LCST region, as expected.

FIGURE 10

THE SHULTZ-FLORY PLOT FOR POLYSTYRENE+HEXANE

The molecular weights are: 2030;4000;
10,000.

T_c is the critical temperature in degrees K,
 r being the ratio of the molar volumes of
the polymer to the solvent.

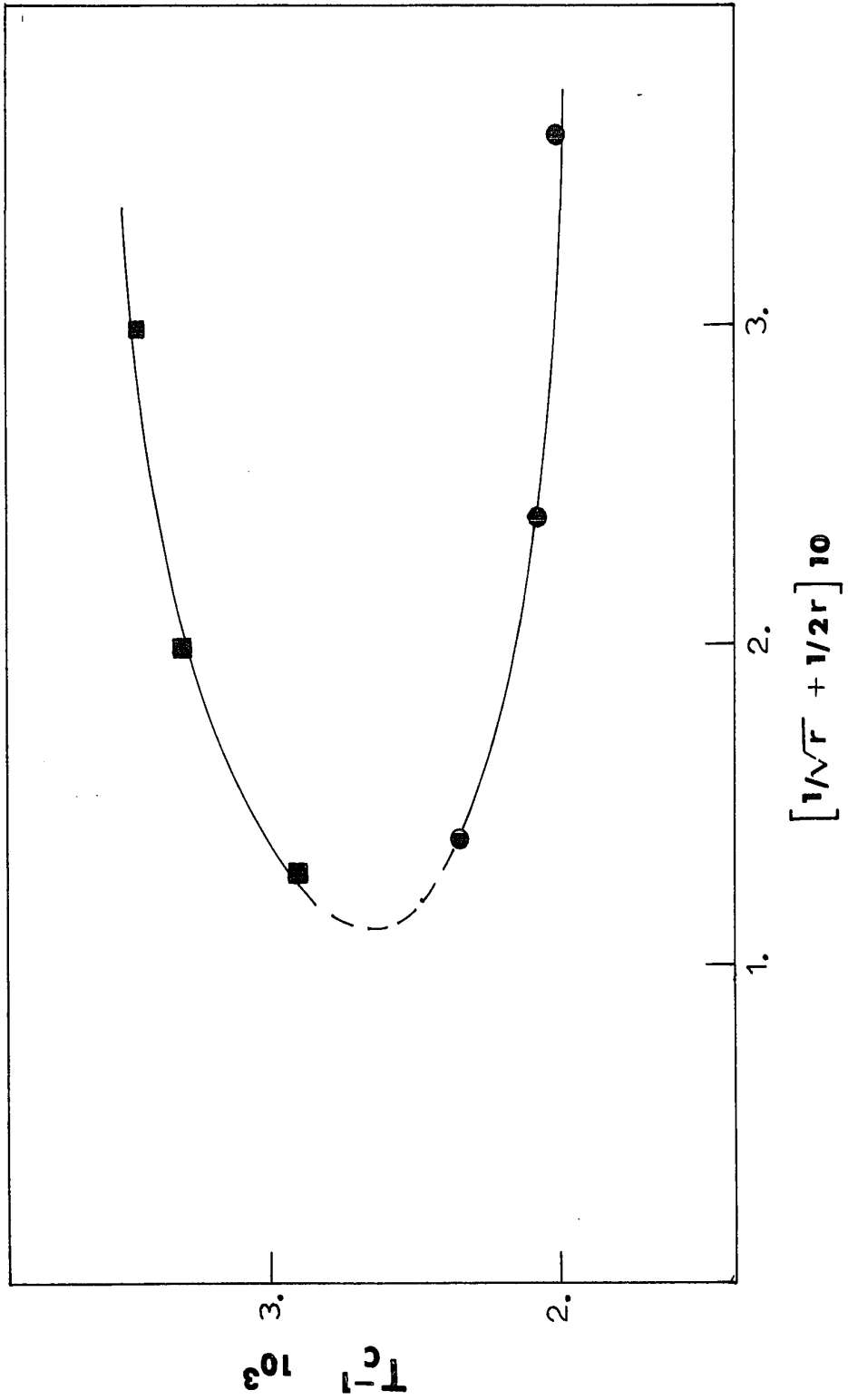


TABLE 4
 VALUES OF THE SLOPE OF THE CRITICAL LINES,
 $(dP/dT)_c$, (bar/deg), AT ZERO PRESSURE FOR PS

Solvent	M	900	2030	4000	10,000	19,800
pentane		-24	-10			
hexane			-28	-28	-8	
dodecane			∞		-380	-65

The two curves, corresponding respectively to the UCST and to the LCST, become one when the UCST and LCST coalesce at the point of infinite slope in Figure 10; this corresponds to a molecular weight of about 13,000. Thus any PS sample having a molecular weight greater than 13,000 behaves in hexane according to the critical line (c) as given in Figure 9.

3. HEATS OF DILUTION OF POLYMER SOLUTIONS

When two non-polar liquids composed of equal-sized molecules are mixed, the heat change (ΔH_M) is almost invariably endothermic. This corresponds to relation 3 which shows that the interchange energy should be positive. However, when small amounts of liquid polymer are mixed, to very great dilution in solvent, there are a number of cases of an exothermic process^{8,9}. This was one of the reasons for the application of the free volume concept to polymer solutions.

It is now well established⁵⁰ that the heat of mixing, ΔH_M , is made up of two terms:

- a "contact interaction term", according to Flory's nomenclature, due to the weakness of (1-2) interactions and expressed by the X_{12} parameter or γ^2 .

- an "equation of state term", due to the dissimilarity of the free volumes of the two components, and associated with the change of \tilde{T} or \tilde{V} from the pure components values to the value in the solution.

The first contribution is positive¹², as expected from the former Flory-Huggins theory. The "free volume" contribution, however, is negative. Thus, if the difference in thermal expansion coefficients between the two components is large enough, the "equation of state term" is predominant, rendering ΔH_M negative.

Although the heat of mixing of a polymer to infinite dilution in a solvent is a quantity of interest, the heat of dilution (or relative partial molar enthalpy) of a polymer

solution is to be preferred. The former quantity shows only the average interaction of the polymer and the solvent as the solution passes from pure polymer to a state of great dilution. The heat of dilution (the heat change of the solution on adding a mole of solvent) may be obtained at any concentration of the solution. The newer theories of polymer solutions predict a change in the polymer-solvent interaction with change of composition and it is therefore of interest to obtain heat of dilution data.

Curiously enough, very few direct measurements of heats of polymer solutions are available, in the literature, for a quantitative test of the "free volume" theories.

3.1 THE HEATS OF DILUTION IN POLYSTYRENE SOLUTIONS

Flory and coworkers¹⁴⁻¹⁷ have been very active in testing the Flory theory¹¹, mainly investigating PIB and PS in a number of solvents. However, the relative partial molar enthalpies, $\Delta\bar{H}_1$, for the solvent, have been obtained through temperature differentiation of the chemical potential, $\Delta\mu_1$.

On the other hand, Johnson and coworkers⁵¹ carried out microcalorimetric measurements on PS+toluene. This latter system shows several remarkable features:

1. the mixing process is exothermic,
2. the enthalpy parameter χ_H (related to $\Delta\bar{H}_1$ by eq. (17)) is strongly concentration dependent, but as will be

discussed below, the sign of the dependence is at variance with predictions by current free volume theories.

3. the molecular weight dependence of the enthalpy parameter does not conform either to the predictions of these theories.

Our own group has been involved in calorimetry for the past few years, the systems studied being PIB in various solvents^{8,39,52}, and PDMS^{39,52,53}. The most striking system is PIB+pentane, for which heats of dilution have been obtained³⁹ over the whole concentration range. The enthalpy parameter χ_H apparently does not depend on concentration, contrary to the predictions of the Flory theory (see Figure 14c).

All these discrepancies prompted us to undertake a systematic study of PS solutions, which show negative heats: PS+toluene, PS+ethylbenzene, PS+2-butanone. In addition, PS+cyclohexane was investigated as a test system for our calorimetric equipment and also because this is a well-known Theta-system. Finally PS+cyclopentane heats were measured for comparison purposes with PS+cyclohexane.

It should be noted that PS at room temperature is not in the liquid state, but is a glass. This lends an additional advantage to heats of dilution rather than of solution. Heats of solution of a polymer have to be measured above the glass transition temperature of the polymer: an exothermic effect⁵⁴ accompanies the dissolution of the polymer in the glassy state.

The dissolution may be considered as the sum of two processes:

1. transition of the glass into the hypothetical liquid polymer below T_g .

2. mixing of the liquid polymer with the solvent.

The heat evolved from the first step would overshadow the comparatively small heat due to the mixing of the liquid polymer with the solvent (step 2).

Heats of dilution circumvent those difficulties; the mixing process occurs between a polymer solution, therefore in the liquid state, and the pure solvent. The obvious drawback is that the determined heats are smaller in this method, requiring more sensitive equipment.

3.1.1 Experimental

3.1.1.1 Materials

Five PS samples were used, four of which were fractions purchased from Pressure Chemical Co., of nominal molecular weight 500; 2,100; 10,000; 51,000. The quoted ratio M_w/M_n was respectively less than 1.10, 1.10, 1.06, 1.06. One PS sample was thermally polymerized* and yielded $M_v = 97,000$. Five solvents were used with one or more of the PS samples. The toluene was a Fisher Certified Reagent of spectrophotometric grade. The cyclohexane was as Spectroquality Reagent

*This sample was polymerized upon our request through the courtesy of Professor Y. Sicotte from the Department de Chimie de l'Universite de Montreal.

from Matheson, Coleman and Bell. The 2-butanone, a Fisher Certified Reagent, and the ethylbenzene, purchased from Eastman Kodak Co., were subjected to column fractionation. Engelhard triple distilled mercury was employed.

3.1.1.2 The Calorimeter

The TIAN-CALVET differential microcalorimeter was found suitable for measuring small heats evolved over a lengthy period of time. Its design is based on Tian's conduction calorimeter⁵⁵; chromel-constantan thermocouples provide pathways for the flow of heat between the reaction cell and a large metal block; the electrical current generated in this thermoelectrical pile is then amplified and recorded.

Our goal was to measure heats of dilution of polymer solutions, at high polymer concentration. However, in this concentration range, the solution becomes very viscous, which makes it virtually impossible to achieve a complete dissolution when the mixing process occurs by gravity, as the case is in the commercial Tian-Calvet differential calorimeter available in this Department.

Professor M. Rinfret, from the Departement de Chimie de l'Universite de Montreal, kindly made available to us his equipment. These calorimeters were built in his Department and are of the Tian-Calvet type. Of interest to us was the feature that the whole calorimeter can be rotated around an

horizontal axle; this simplifies the otherwise difficult mixing process and makes it much more efficient, particularly at high polymer concentration. In addition, the temperature of the metal block in this calorimeter is set by a water bath, regulated at $\pm 0.01^{\circ}$ (at 25° in our experiments), the water running through metal pipes inside the calorimeter.

The thermocouples are regularly embedded around the measuring cell and the reference cell, wired so as to constitute two thermopiles connected in opposition. This gives a perfectly stable experimental base line over a long period of time, because it does not require a fixed temperature but only the same temperature at a given time throughout the aluminium block. The signal, carried through conduction wires positioned in the shaft, is fed into an amplifier (Keithley), the output of which is recorded on a Philips, model PR 3216, potentiometric recorder. Only two out of the twelve channels available were used alternatively: one for the signal of the calorimeter, the other giving the zero of the recorder.

3.1.1.3 The Cell

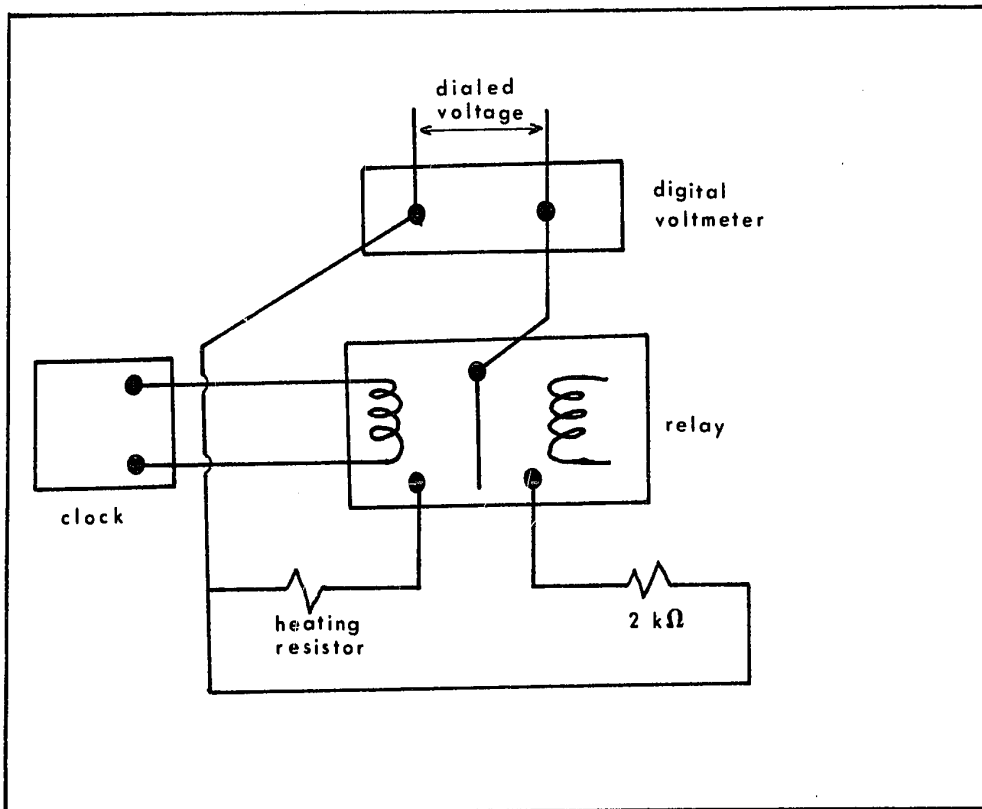
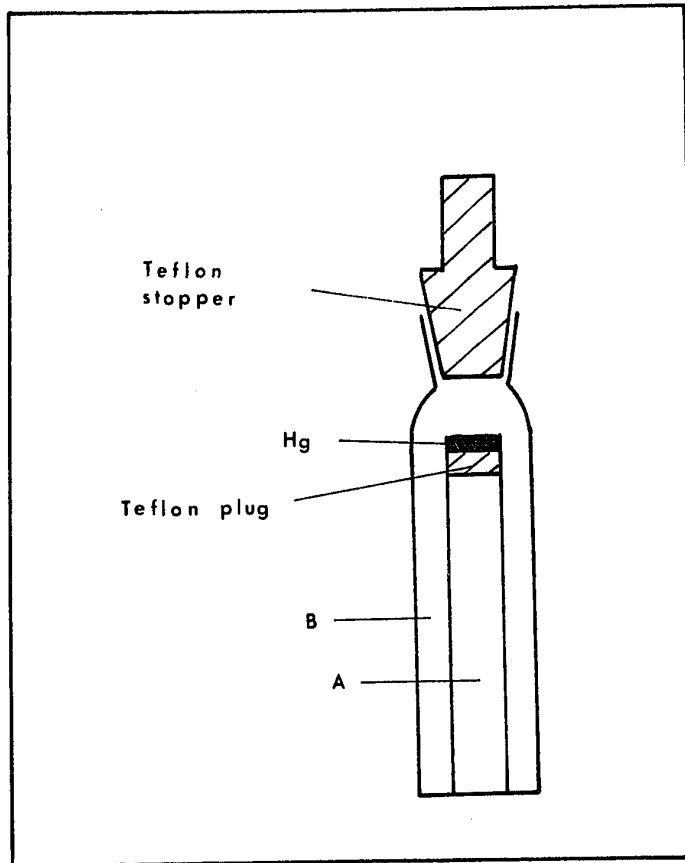
A cross section view of the cell is given in Figure 11. The body of the cell is made of Pyrex and is cylindrical in shape. The total volume available to the solution is about 25 cm^3 . The inner compartment (A) is closed by a Teflon cap seated on a Teflon gasket; mercury sealed off this part from the outer compartment (B). A Teflon stopper closed off the cell.

FIGURE 11

CROSS SECTION VIEW OF THE CALORIMETER CELL

FIGURE 12

EXPERIMENTAL SET-UP FOR CALIBRATIONS



3.1.1.4 Procedure

Filling procedure of the cell. The quantities of material used for each experiment were weighed on a Sartorius balance. First a solution was prepared. Then the inner compartment was filled with solvent, using a regular syringe. Special care had to be taken to avoid any spill-over in the outer compartment of the cell. The Teflon cap was put into place and about 0.5 cm^3 mercury was added. Next the polymer solution was added into the outer compartment. It is important not to leave any vapour space, therefore the level had to be carefully adjusted; however this was done at a temperature below 25° , and usually at temperature equilibrium, the vapour space was minimal. The polymer solution was always placed in the outer compartment for two reasons:

- the filling process is simplified,
- the mixing process starts faster.

No grease was used on the Teflon stopper because of the heat which might have been given off due to the grease dissolution or interaction with the solvent. Sealing was realized by pressing tightly the stopper against the ground glass. Any evaporation of volatile solvent gives rise to drifting, or shifting of the base line, and is therefore easily detectable. The cell was then carefully inserted into the calorimeter, and tightened in the cavity so that no heat would arise from friction during the dilution process.

Attainment of temperature equilibrium took $1\frac{1}{2}$ hour. The thermal stability of the system is verified by the linearity of the base line. Once a straight line is obtained, the cell is fired by switching on the rotation system. The dilution process was $1\frac{1}{4}$ hour long in a typical experiment. The chart speed was set at 300 mm/hour.

The calorimeter was tilted between 45 and 135° angle (with reference to the vertical position) continuously during the experiment, at a speed of about 1 period per mn.

The heat ΔH_d , evolved during the dilution is determined by measuring the area under the curve with a planimeter and by calibrating the instrument. During the dilution, the polymer solution of initial concentration ϕ_2^i arrives at a final concentration ϕ_2^f by addition of Δn_1 moles of solvent. Integration of eq. (17), keeping χ_H constant, yields ΔH_d :

$$\Delta H_d = RT \chi_H \phi_2^i \phi_2^f \Delta n_1 \quad (34)$$

with

$$\phi_2 = \frac{w_2 v_{2,sp}^*}{w_1 v_{1,sp}^* + w_2 v_{2,sp}^*} \quad (35)$$

It is known however that χ_H may vary with concentration⁵⁶. A value of χ_H is found through applying eq. (34) to a measured value of ΔH_d . However, it is only an average or apparent value, $\chi_{H,app}$. The concentration dependence of χ_H may be represented by the following expression:

$$\chi_H(\phi_2) = \chi_{H,1} + \chi_{H,2} \phi_2 + \chi_{H,3} \phi_2^2 + \dots \quad (36)$$

Terms beyond $\chi_{H,3}$ may be neglected and in fact $\chi_{H,1}$ and $\chi_{H,2}$ give a satisfactory representation of most results. If this expression is substituted into eq. (17), a new relation for ΔH_D is found. It may be compared with eq. (34) so that the following significance is given to $\chi_{H,app}$:

$$\begin{aligned} \chi_{H,app} = & \chi_{H,1} + \chi_{H,2} \phi_2^a + \chi_{H,3} (\phi_2^a)^2 \\ & + \chi_{H,3} \left(\frac{\phi_2^f - \phi_2^i}{12} \right)^2 + \dots \end{aligned} \quad (37)$$

where ϕ_2^a is the arithmetic mean of ϕ_2^i and ϕ_2^f .

In the present work, $\phi_2^f - \phi_2^i$ is less than or equal to 0.1, thus rendering negligible the last term in eq. (37). Accordingly, $\chi_{H,app}$ is not different from χ_H at the mean segment fraction ϕ_2^a .

3.1.1.5 Calibration

The Joule effect is a convenient source for the heating power needed for the calibration. The resistor in the reference cell is immersed in paraffin and has been measured using a capacitor bridge; the value, R , was found to be $1952.0 \pm 0.2 \Omega$. The resistance of the conduction wires, of the order of 0.2Ω was neglected. A digital voltmeter feeds into the resistor a constant pre-set voltage during t seconds.

The timing is controlled by an electronic clock, as seen in Figure 12. The heat emitted at the resistor, $V^2/R \cdot t$, divided by the area under the recorded curve, yields the calibration constant in cal/cm^2 . A calibration has been carried out for each amplification gain. The calibration constants are listed in Table 5, each one being an average of four determinations.

TABLE 5
TIAN-CALVET DIFFERENTIAL CALORIMETER
CALIBRATION CONSTANTS AT 25°

sensitivity range (mv)	0.01	0.03	0.1	0.3	1.0
$10^3 \times$ heat/surface (cal/cm^2)	2.46	7.46	24.6	75.1	246.7

3.1.1.6 Sources of Error, Precision and Accuracy

The reproducibility can be estimated by comparing the results, i.e. surfaces, obtained in the calibration experiments. For every amplifier gain, the average absolute deviation (centered moment of 1st order) is in between 0.1 and 0.9 cm^2 , the surfaces measured being 100 cm^2 approximately. Obviously the differences are due to errors incurred while measuring those surfaces.

Systematic errors which may influence the accuracy of the measurements are⁵⁵:

- irregular distribution of the thermocouples around the cells.

- heat loss from the upper part of the cell which is not covered by thermocouples.

- the thermocouple assemblies for the measuring cell and the reference cell are different, and temperature fluctuations could therefore cause errors in the determination of the heats.

Accidental causes of errors are as follows:

- evaporation of the solvent, which has been dealt with in section 3.1.1.4.

- the heat evolved by the mercury and the "rocking" was detectable only at the highest sensitivity; this is seen by the base line which has been shifted, and therefore the correction can be easily made.

- bad electrical contacts, detected by checking the "zero" of the amplifier against the "zero" of the calorimeter.

- vapour space correction, required whenever vapour space is left over the polymer solution. Senez and Daoust⁵⁷ give the limits of the correction. The heat due to vapour space was calculated for PS+2-butanone and found less than 6×10^{-4} cal whereas the heat of dilution was -0.05 cal. This

is negligible and confirmed our experimental investigation: a change of vapour space from "zero" to about 1 cm^3 gave values of χ_H within experimental errors.

- a shift of the base line taking place during an experiment. This results in an uncertainty when small heats are measured.

- an uncertainty in the value of the calibration constant which has its source mainly in the different thermokinetic profile of a calibration curve and a heat of dilution curve. In addition, the calibrations are done with exothermal heats.

- the planimeter's reproducibility is within 0.5%.

The accuracy and precision are believed to be of the same order of magnitude, and are given in the various Figures.

3.1.2 Results

Figures 13a,b,c and 14a, b show respectively the values of the enthalpy parameter χ_H as a function of ϕ_2 , the segment fraction of the polymer, for different molecular weight of PS in cyclohexane, cyclopentane, 2-butanone, toluene and ethylbenzene at 25.0° . The χ_H values were calculated from the heats of dilution, ΔH_d , using eq. (34). The abscissa, ϕ_2 , is the arithmetic mean segment fraction of the initial and final concentrations. In addition, the theoretical predictions,

FIGURE 13

THE ENTHALPY PARAMETER, $\chi_H = \Delta\bar{H}_1/RT\phi_2^2$ AS A FUNCTION OF THE SEGMENT FRACTION, ϕ_2 , AT 25°, FOR

- a) PS+CYCLOHEXANE
- b) PS+CYCLOPENTANE
- c) PS+2-BUTANONE

The continuous lines have been calculated from theory for a temperature of 25°. The various PS molecular weight fractions are:

open circles	600
closed circles	2100
open squares	10,000
closed squares	20,400
open triangles	51,000
closed triangles	97,000

The results of Lam⁵⁹ have been plotted: half closed circle: 4,000 and half closed triangle: 97,000.

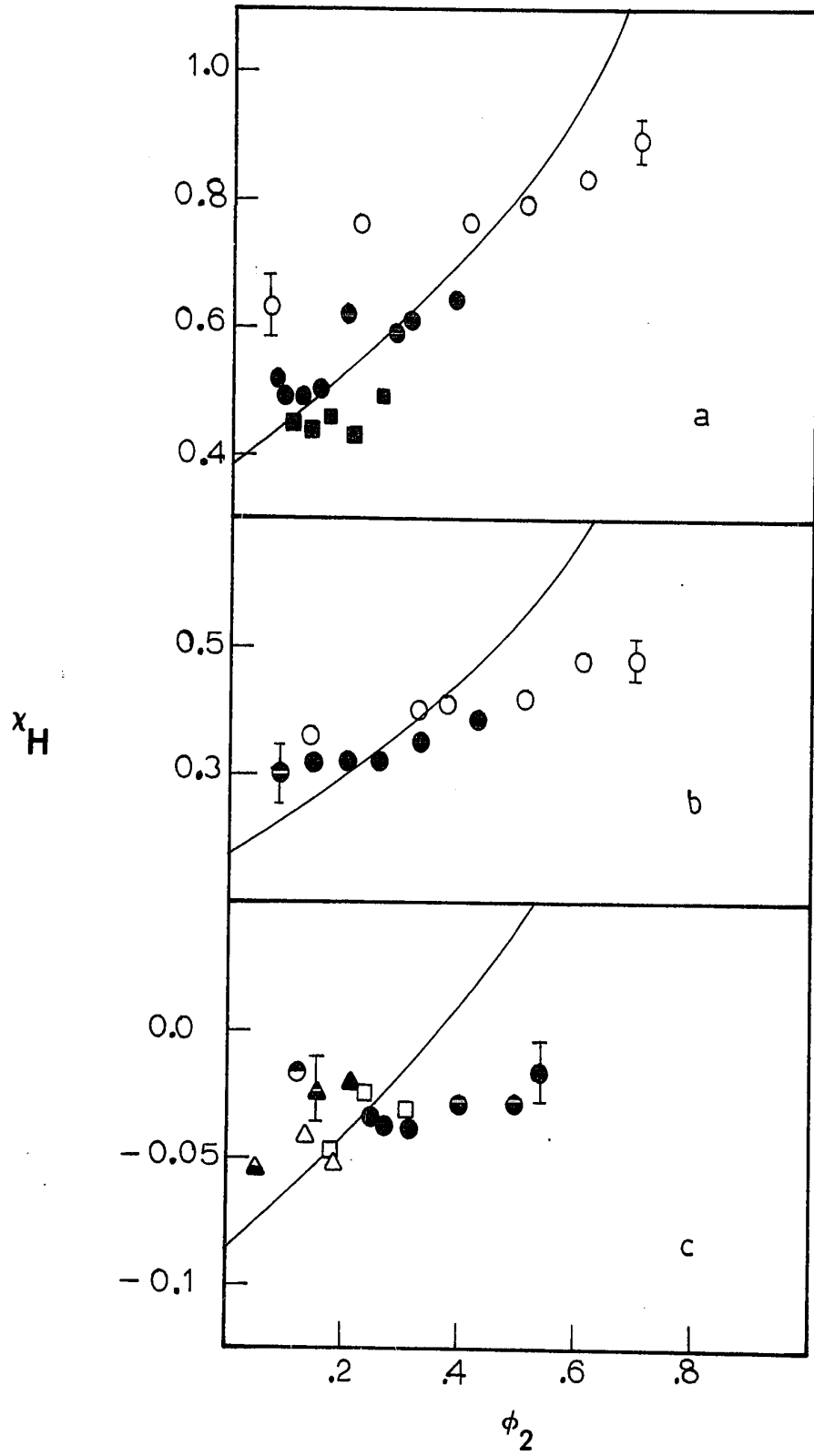


FIGURE 14

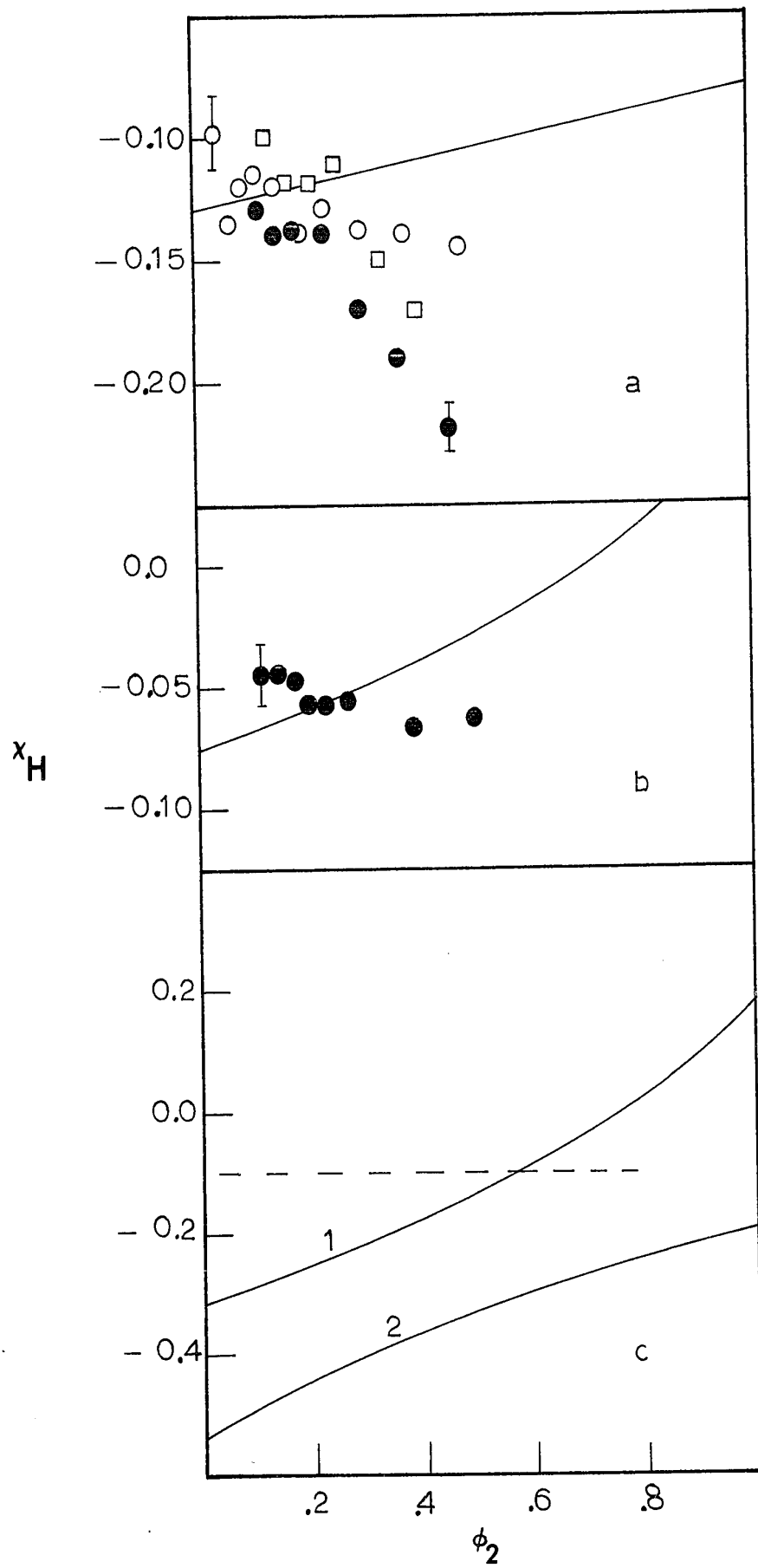
THE ENTHALPY PARAMETER $\chi_H = \Delta\bar{H}_1/RT\phi_2^2$ AS A FUNCTION OF THE SEGMENT FRACTION ϕ_2 , AT 25°, FOR

- a) PS+TOLUENE
- b) PS+ETHYLBENZENE
- c) PIB+n-PENTANE

The continuous line has been calculated from theory for a temperature of 25°. The various PS molecular weight fractions are:

open circles	600
filled circles	2100
open squares	10,000
filled squares	20,400
open triangles	51,000
filled triangles	97,000

The broken line of (c) are the data from ref. 39. Curve (1) has been calculated with $\chi_{12} = 2.8 \text{ cal/cm}^3$, and curve (2) with $\chi_{12} = 0.25 \text{ cal/cm}^3$.



according to the Flory theory, are given for each system and are represented by the continuous lines.

The expression for the heat of dilution, as given by the Flory theory is^{14a}:

$$\begin{aligned} \Delta\bar{H}_1 = & p^*_1 v^*_1 [\tilde{V}_1^{-1} - \tilde{V}^{-1} + (\frac{\alpha T}{\tilde{V}}) (\frac{\tilde{r}_1 - \tilde{r}}{\tilde{r}})] \\ & + \frac{v^*_1 X_{12}}{\tilde{V}} (1 + \alpha T) \theta_2^2 \end{aligned} \quad (38)$$

Here the star and tilde signify respectively reduction parameters and reduced quantities. The subscripted quantities correspond respectively to component 1, the solvent, and component 2, the polymer. T is the temperature at which the mixing takes place. The reduced, non-subscripted variables correspond to the solution. In this expression, the two contributions to the heat of dilution, $\Delta\bar{H}_1$, are, as usual, the equation of state and the contact interaction terms, represented respectively by the three first terms in the square brackets and by the last one. The parameter θ_2 is the surface fraction, related to the segment fraction by:

$$\theta_2 = \frac{s_2 \phi_2}{s_1 \phi_1 + s_2 \phi_2} \quad (39)$$

where s_i represents the molecular surface to volume ratio of component i.

It has always been a difficulty in free volume theories, for mixtures of non-homologs, to determine accurately the parameter which reflects the "chemical difference" of the two components, i.e. χ_{12} or γ^2 . Usually a fitting is done, as in section 2.1.3.3. In the present case, a value of χ_{12} was determined by fitting eq. (38) to experiment at a single concentration. Then $\Delta\bar{H}_1$ and χ_H were determined from eq. (38) and (17) at other concentrations. In addition, χ values were calculated using eq. (48) of ref. 14a, and χ_S was then obtained with eq. (4). The results are given in Table 6. The molecular parameters required for the calculations are summarized in Table 7. The values for PS+ethylbenzene, +cyclohexane, +2-butanone were taken from Flory et al.^{15-17,58} for comparison purposes. In the case of PS+cyclopentane and PS+toluene, values of s_2/s_1 , the ratio of the surface to volume ratios for the polymer and the solvent,

were not available and had to be calculated according to Flory's recommendation¹⁵. Assuming the sphericity of the solvent molecule, the molecular surface to volume ratio, S/V^* , for the polymer segment, PS, was obtained and found equal to 0.47 (by taking either of the three systems investigated by Flory). Next S/V^* values were obtained for cyclopentane and toluene, yielding s_2/s_1 ratios for those two systems.

The heats of dilution for PS+2-butanone are very small but were confirmed by microcalorimetry by another author⁵⁹.

TABLE 6
CALCULATED χ , χ_H AND χ_S AT 25° ACCORDING TO
THE FLORY THEORY

<u>ϕ_2</u>	<u>χ</u>	<u>χ_H</u>	<u>χ_S</u>
<u>PS+CYCLOHEXANE</u>			
0.10	0.461	0.726	0.264
0.20	0.530	0.794	0.263
0.30	0.613	0.874	0.260
0.48	0.712	0.969	0.257
0.50	0.830	1.083	0.253
0.60	0.973	1.222	0.249
0.70	1.150	1.394	0.243
0.80	1.372	1.609	0.236
0.90	1.657	1.885	0.228
1.00	2.031	2.247	0.216
<u>PS+CYCLOPENTANE</u>			
0.10	0.235	0.658	0.423
0.20	0.295	0.714	0.419
0.30	0.365	0.780	0.415
0.40	0.447	0.858	0.411
0.50	0.545	0.953	0.408
0.60	0.665	1.070	0.405
0.70	0.813	1.215	0.402
0.80	1.000	1.399	0.398
0.90	1.243	1.638	0.394
1.00	1.567	1.957	0.389
<u>PS+2-BUTANONE</u>			
0.10	-0.063	0.400	0.463
0.20	-0.042	0.422	0.464
0.30	-0.017	0.448	0.465
0.40	0.010	0.478	0.468
0.50	0.043	0.514	0.471
0.60	0.081	0.557	0.475
0.70	0.128	0.609	0.480
0.80	0.187	0.673	0.486
0.90	0.262	0.755	0.493
1.00	0.360	0.862	0.501

TABLE 6 (cont'd)

<u>ϕ_2</u>	<u>χ</u>	<u>χ_H</u>	<u>χ_S</u>
<u>PS+TOLUENE</u>			
0.10	-0.123	0.248	0.371
0.20	-0.119	0.253	0.372
0.30	-0.115	0.258	0.373
0.40	-0.110	0.263	0.373
0.50	-0.105	0.269	0.376
0.70	-0.096	0.282	0.379
0.80	-0.091	0.290	0.382
0.90	-0.085	0.300	0.385
1.00	-0.079	0.310	0.390
<u>PS+ETHYLBENZENE</u>			
0.10	-0.065	0.275	0.341
0.20	-0.058	0.283	0.342
0.30	-0.049	0.292	0.342
0.40	-0.039	0.303	0.342
0.50	-0.027	0.314	0.342
0.60	-0.014	0.328	0.343
0.70	0.000	0.344	0.344
0.80	0.018	0.364	0.345
0.90	0.040	0.387	0.346
1.00	0.068	0.416	0.348

TABLE 7

PURE COMPONENT AND SOLUTION PARAMETERS AT 25°

SYSTEM	$\alpha_1 \cdot 10^3$ (deg. ⁻¹)	$\alpha_2 \cdot 10^3$ (deg. ⁻¹)	V_1^* (cm ³ /mole)	$v_{2,sp}^*$ (cm ³ /g)	P_1^* (cal/cm ³)	P_2^* (cal/cm ³)	s_2/s_1	X_{12} (cal/cm ³)
PS+toluene	1.077(1)	0.572(3)	84.58(1)	0.8098(3)	134.0(1)	130.7(3)	0.51	0.15
PS+ethylbenzene	1.019(2)	0.572	98.33(2)	0.8098	131.7(2)	"	0.53(2)	0.96
PS+2-butanone	1.308(3)	"	68.94(3)	"	139.1(3)	"	0.48(3)	0.40
PS+cyclohexane	1.217(4)	"	84.26(4)	"	126.6(4)	"	0.50(4)	15.05
PS+cyclopentane	1.390(5)	"	71.61	"	128.4	"	0.48	14.16

- (1) see ref. 62
 (2) see ref. 16
 (3) see ref. 15
 (4) see ref. 17
 (5) see ref. 63

For cyclopentane, V^* has been calculated using $\rho = 0.74045 \text{ g/cm}^3$ (ref. 64), and P^* using $\beta = 1.37 \times 10^{-4} \text{ atm}^{-1}$ (ref. 65).

3.1.3 Discussion

PS+CYCLOHEXANE

Three PS fractions, of molecular weight 600, 2,100 and 20,400, were studied in cyclohexane. The two lower molecular weight samples show a similar behaviour over a large concentration range. As expected, χ_H is positive and large, and increases drastically with the concentration. The Flory theory gives a very good prediction, particularly in the first half of the concentration range. Earlier investigations, carried out over a wide concentration span by Krigbaum et al.⁶⁰ and Scholte⁶¹ agree well with our own data, if the molecular weight dependence is taken into account. Particularly in the case of the isothermal distillation data, the slope of (χ_H, ϕ_2) increases drastically above $\phi_2 = 0.50$ which compares very well with the calculated χ_H values given in Figure 13a. Our fitted χ_{12} value was equal to 15.1 cal/cm³, whereas Flory gives about 10.0 cal/cm³ (p. 2278 of ref. 17). This is due to a different value of χ_H at which the fitting took place; this accounts also for our steeper predicted χ_H curve. The interaction parameter χ was calculated using our χ_{12} value, at various concentrations as listed in Table 6. Apparently the χ values are very large and probably too much concentration dependent from 0.73 to 2.3. On the other hand, the entropy parameter, χ_S , remains constant through the whole concentration span, reflecting the similarity of the

concentration dependences of χ_H and χ .

The PS+cyclohexane system, together with PIB+benzene, are probably the most standard systems in polymer solution thermodynamics. Daoust and Kabayama⁵⁶ have made an extensive calorimetric investigation of the heats of dilution of the latter system. Since no similar study had been made of PS+cyclohexane, we were interested to do so. The two systems are similar. Both have Theta points near room temperature, 34° for PS+cyclohexane and 25° for PIB+benzene. Both systems are strongly endothermic at room temperature, reflecting the proximity of the Theta point and the difference between the aromatic and aliphatic characters of the components. In both cases, χ_H increases rapidly with increasing polymer concentration. Since the Flory theory is successful in predicting the concentration dependence, one must conclude that the physical reason given by the theory for the concentration dependence is probably correct. The reason is that most of the heat effect is due to the positive endothermic "contact interaction" contribution to $\Delta\bar{H}_1$. Theoretically, this contribution depends, not on the volume fraction or segment fraction ϕ_2 of the polymer, but on the fraction of total molecular surface which belongs to the polymer, i.e. the surface fraction θ_2 . Thus $\Delta\bar{H}_1 \propto \theta_2^2$, but in the conventional relation for the heat of dilution, χ_H is defined in terms of ϕ_2 :

$$\Delta\bar{H}_1 = \chi_H RT \phi_2^2$$

Therefore, χ_H must vary as:

$$\chi_H \propto (\theta_2/\phi_2)^2$$

introducing the surface to volume ratios of the components as given by eq. (39). When $\phi_2 \rightarrow 1$, the ratio $\frac{\theta_2}{\phi_2} \rightarrow 1$; on the other hand, when $\phi_2 \rightarrow 0$, $\frac{\theta_2}{\phi_2} \rightarrow s_2/s_1$. If $s_2/s_1 < 1$, a decrease of χ_H will occur as $\phi_2 \rightarrow 0$. This is the reason for the decrease of χ_H in the PS+cyclohexane system.

PS+CYCLOPENTANE

The two molecular weight PS fractions investigated, 600 and 2,100, gave a concentration dependence of χ_H very similar to the preceding system. The theoretical predictions are again in reasonable agreement up to a segment fraction of 0.50, after which the increase is too large for the predicted χ_H . Our fitted χ_{12} value was found to be equal to 14.2 cal/cm³. The interaction parameter χ was calculated using this value of χ_{12} and is listed in Table 6 for various concentrations. Again the concentration dependence of χ is very large, from 0.66 to 1.96. The entropy parameter is concentration independent and remains at 0.40.

Here the interesting point is that the cyclopentane molecule is of the same "chemical character" as cyclohexane, but of a quite different shape. Benson and collaborators have

found that the thermodynamics of decalin+cyclopentane⁶⁶ is quite different from that of decalin+cyclohexane⁶⁷, and that this change may be attributed to the change in shape of the cyclo-alkane. However, in the present case, reasonable agreement between theory and experiment is still found using the Flory theory, without allowing for any difference of molecular shape.

The three systems studied below are of interest since the heats are exothermic. Here, the free volume contribution is dominant.

PS+2-BUTANONE

The light scattering data obtained by Zimm and coworkers⁶⁸ in very dilute solutions yield negative values of the heat of dilution, $\Delta\bar{H}_1$. Bawn and Wajid⁶⁹, and Doty and coworkers⁷⁰ have obtained small negative heats of dilution at concentrations up to 0.10 in volume fraction. At higher concentration of polymer, Bawn et al.⁷¹ found by vapour pressure measurements a small positive heat. However, they suggest not to use their results of $\Delta\bar{H}_1$ for further thermodynamic derivations: their determination, they claim, was not accurate enough. Flory¹⁵, nonetheless, used those results to calculate the concentration dependence of χ_s and compare it with his own predictions.

Kagemoto and coworkers⁷² measured heats of dilution at concentrations up to 0.2 in volume fractions, and found endothermic heats. Our results in Figure 13c, show small negative values of χ_H . The enthalpy parameter does not show any concentration dependence in the range of ϕ_2 equal to 0.10 up to 0.50 which has been studied, and therefore the same behaviour is expected in the high polymer concentrations. The discrepancy between Kagemoto's and our results can not be explained in terms of the tacticity of our PS samples since one PS fraction was thermally polymerized to circumvent this difficulty: no difference in the heats was found.

The theoretical predictions yield a curve of positive slope, our value of χ_{12} being equal to 4.4 cal/cm³ which compares well with Flory's 6.2 cal/cm³. The theoretical predictions of the interaction parameter χ , agree very well with the data of Bawn et al.⁷¹. This is not the case for χ_S which is predicted to be constant almost at about 0.48.

In conclusion, it is seen for this system that the concentration dependence of χ_H is not predicted. The Flory theory gives increasing χ_H values as the polymer concentration is raised, whereas the χ_H , measured calorimetrically, is insensitive to any concentration changes.

PS+ETHYLBENZENE

Pouchly and coworkers²⁴, by calorimetry, found the enthalpy parameter to be negative. Palmen's data, treated by Flory¹⁶ at ϕ_2 equal to 0.10, yield a small but negative value for χ_H . These results are consistent with our own calorimetric heat of dilution determinations. Maron et al.⁷³ found the heats of dilution essentially equal to zero for this system. Their determinations were probably approximate only, in view of the purpose of the measurements. Figure 14b shows that the enthalpy parameter is always negative, and moreover becomes smaller as the concentration of polymer is increased. However, the predicted curve does not follow the same pattern. The slope is positive and the χ_H values become positive above ϕ_2 equal to 0.70. The fitting was performed with an χ_{12} value equal to 1.0 cal/cm³, reflecting the "chemical similarity" of the two components. The χ values generated by the same procedure vary from 0.28 to 0.42, in good agreement with the osmometry data of Flory et al.¹⁶ who used higher molecular weight PS. χ and χ_H having the same concentration dependence, χ_S is constant over the whole concentration span.

The same conclusion, given for PS+2-butanone, is reached for this system: theory and experiment disagree upon the concentration dependence of the enthalpy parameter, χ_H .

PS+TOLUENE

This system has been studied by a number of authors. Schick, Doty and Zimm⁷⁰ found a negative heat of dilution by osmometry. However, the concentration dependence shows an upward trend and should lead to positive χ_H values above volume fractions of 0.10. Bawn and Wajid⁶⁹ and Bawn, Freeman and Kamaliddin⁷¹ found $\Delta\bar{H}_1$ equal to zero throughout the whole concentration range. Schmol1 and Jenckel⁷⁴, by vapour pressure measurements, found the enthalpy parameter to be zero within experimental error. Scholte⁶¹, by sedimentation, found χ_H to be negative at concentrations up to 90% in weight.

Calorimetric data have been reported. Kagemoto and coworkers⁷² give the concentration dependence of the enthalpy parameter: χ_H varies from -0.05 to -0.20 for a volume fraction increasing from 0.02 to 0.15. This compares well with our results given in Figure 14a. Maron⁷³ gives again a zero value for the heat of mixing, which has to be discounted for the reason mentioned above. Johnson⁵¹ investigated this system thoroughly, and his results are consistent with our data. However, we did not find any significant increase of the absolute value of χ_H for the 600 molecular weight fraction, when the concentration decreases below $\phi_2 = 0.10$. But the main feature, the negative slope of the (χ_H, ϕ_2) plot, is confirmed in our experiments over a wider concentration range, up to $\phi_2 = 0.50$. The solid curve in Figure 14a has been calculated

using an χ_{12} value equal to 0.15 cal/cm^3 . It is located in the negative values of χ_H , however the slope is still positive. If one were to use an unrealistic negative value for χ_{12} , the slope could be made equal to zero or even slightly negative, but in doing so the curve would be lowered and hardly be called a fit any more. The χ values are predicted reasonably well and vary from 0.25 to 0.31 over the whole concentration range. Those low χ values reflect the "goodness" of the solvent. On the other hand, χ_S is almost concentration independent and remains equal to 0.38.

Apparently, the behaviour of the five systems investigated, can be summarized by classifying them into two groups:

1. PS+cyclohexane and +cyclopentane exhibit endothermic heats, and the concentration dependence of their enthalpy parameter is positive and well predicted according to free volume theories.

2. PS+2-butanone, +ethylbenzene and +toluene are exothermic systems in nature and their respective $d\chi_H/d\phi_2$ are zero and negative, and can not be predicted by the Flory theory. The system PIB+pentane fits into that second group: $d\chi_H/d\phi_2$ has been found essentially zero³⁹ and is not predicted correctly.

The surface to volume ratio of the two components is a parameter which influences the concentration dependence of χ_H .

This has been noticed by Flory¹⁵. The use of volume and surface increments, advocated by Bondi⁷⁵, leads always to s_2/s_1 values in the range of 0.9 to 1.0. The χ_H versus ϕ_2 curves were generated in the way described above, using surface to volume ratios calculated according to Bondi. The curves obtained have smaller slopes, thus improving a little the general picture. The s_2/s_1 values, however, are unrealistic because the recipe overestimates the surface of the polymer available to the solvent for the interactions. It does not allow for any loss of polymer surface, arising from polymer adjacent segments being in contact. Flory¹⁵, on the other hand, considers the polymer as a cylinder of known dimensions and the solvent molecule is assimilated to a sphere. This recipe leads always to a surface to volume ratio equal to approximately 0.5 (see column 8 of Table 7), which brings in a larger concentration dependence of χ_H .

It may be argued that, the Flory theory being, formally at least, a particular case of corresponding states theory⁵⁰, another potential model would give better results than the $(3, \infty)$ potential model to which the Flory theory can be equated within the corresponding states theory. However, it turns out that the sign of $d\chi_H/d\phi_2$ does not change with the model used.

Patterson⁷⁶, by use of a corresponding states approach, gives the following expression of $dx_H/d\phi_2$ or

$$K_2 \equiv \chi_{H,2}$$

$$K_2 \equiv \chi_{H,2} = \frac{TdC_p/dT}{R} \gamma^2 \tau + \frac{Td^2C_p/dT^2}{3R} \tau^3 \quad (40)$$

The second term in this relation is always positive because of the curvature of the (C_p, T) function. On the other hand, the first term, in which appears the "chemical difference" parameter, γ , may be positive or negative. In any case, when χ_{12} is small (or γ), the first term in the relation (40) vanishes, and $dx_H/d\phi_2$ has to be positive for the PS+toluene and PS+ethylbenzene systems.

Therefore the concentration dependence of the enthalpy parameter χ_H appears to indicate a failure of the corresponding states principle as applied to polymer solutions. The same failure has been found in other polymer solution work⁵². This discrepancy between theory and experiment, particularly for systems where the free volume contribution is predominant, led us into the investigation of mixtures of low molecular weight model compounds. This should provide an answer to the question as whether the corresponding states principle still applies to mixtures of shorter chain molecules as opposed to polymer solutions. However we avoided PS

models²⁴ and studied the commercially available PIB models. We remember that the discrepancy between theory and experiment is found, not only with PS solutions, but also the PIB in pentane and PDMS solutions³⁹.

3.2 THE HEATS OF MIXING OF THE LOW MOLECULAR WEIGHT COMPOUND MIXTURES

The preceding section was concluded by stating the failure of the corresponding states principle as applied to polymer solutions. If instead of a polymer, as component 2 in the solution, one uses a low molecular weight model or an oligomer of the macromolecule, only the free volume term in the mixing functions changes. Indeed, it is known that the end-effects have been overestimated⁵², leaving therefore the chemical difference (X_{12} or γ^2) invariant when a polymer is substituted by its oligomer. The oligomer which was chosen is a branched alkane: 2, 2, 4, 4, 6, 8, 8-heptamethylnonane, called "iso-C16" for brevity in the text, and which is a tetramer of PIB.

3.2.1 Experimental

3.2.1.1 Materials

The liquids were used without further purification, their quoted specifications and sources are listed in Table 8. Engelhard triple distilled mercury was used without further purification.

TABLE 8
ORIGIN AND SPECIFICATIONS OF THE LIQUIDS USED
FOR HEAT OF MIXING EXPERIMENTS

<u>LIQUIDS</u>	<u>MANUFACTURER</u>	<u>SPECIFICATIONS</u>
2,2,4,4,6,8,8-heptamethylnonane	Aldrich Chemical Co.	98%
n-hexadecane	"	spectrophotometric grade
2,2,4,-trimethylpentane	Matheson, Coleman and Bell	spectroquality 99%
2,2-dimethylbutane	Phillips	research grade 99.96%
n-hexane	"	" " 99.99%
n-pentane	Matheson, Coleman and Bell	spectroquality 99%
benzene	"	" "
carbon tetrachloride	Baker Chemical Co.	"
cyclohexane	Matheson, Coleman and Bell	" 99%

3.2.1.2 The Calorimeter

The microcalorimeter employed was a CRMT model commercialized by SETARAM (Lyon, France). It is essentially a smaller replica of the Tian-Calvet microcalorimeter, described in section 3.1.1.2, less accurate but easier to use. The CRMT is not a differential but a monocell calorimeter. The thermocouples are of the same nature and number as in the Tian-Calvet model. This model is supplied (contrary to the Tian-Calvet model) with a mechanism which rotates the whole calorimeter at 1 cycle per mn around an horizontal shaft by 180° from the vertical position. The advantage of this motion for the mixing process has been discussed previously. The temperature of the calorimeter is regulated, within 0.1° , by an built-in temperature controller, and was continuously checked by measuring a resistance planted in the metal block. The signal of the calorimeter is fed directly, without further amplification in our case, into a galvanometric recorder (Graphispot, SEFRAM, Paris).

3.2.1.3 The Cells

The cells have the same basic design as shown in Figure 11, because the mixing process will be the same. It is a "2 compartment" cell, the body being cylindrical, made of stainless steel and threaded at both ends. The two compartments are separated by a stainless steel tube, attached to the bottom

of the cell. Bottom and top parts were Teflon screws. The inner compartment is sealed off by means of a steel plate. Five cells, having a different volume ratio of the inner and outer compartments, were used, thus covering the whole concentration range. The total volume accessible to the liquids was about 10 cm^3 .

3.2.1.4 Procedure

The filling procedure of the cell is essentially the same as described in section 3.1.1.4. The inner compartment is filled first by means of a syringe, the cover is put into place and the excess liquid is dried away. No vapour space is left. Next, the bottom part with the inner cell attached, is screwed carefully to the main body, and about 0.5 cm^3 of mercury is added on top. Then the second component is added and the top part is screwed tightly. The excess of the second component came out through the threads while closing the cell. Again no vapour space is left in the cell. The amount of each liquid in the cell is known by weight (before and after the liquids are added). The cell is then carefully inserted into the cavity of the calorimeter and tightly held in order to avoid any heat effect produced by friction while the instrument is tilted up and down. About $1\frac{1}{2}$ hour is allowed for reaching temperature equilibrium. As usual, the thermal stability of the instrument is verified by observation of the

base line of the recorder. Once the base line is completely linear, the chart speed is set on 360 mm/hour and the cell is fired by switching on the rotation system. The calorimeter is continually rotated during the whole experiment, lasting about 3/4 hour, and stopped when the recorder's pen is back in the position of the original base line (before the cell was fired). It should be mentioned that the heat produced by the mercury during the rocking was not detectable on any sensitivity.

Finally the heat of mixing is determined by measuring the area under the curve and with the calibration constant of the instrument. Usually one expresses the results in cal/mole obtained by dividing the actual heat in cal (obtained as mentioned above) by the total number of moles of the two components.

3.2.1.5 Calibrations

The procedure, as given in section 3.1.1.5, is followed. Heat is developed by Joule effect in a special resistor, supplied by the manufacturer SETARAM, of known resistance, equal to $1,000 \pm 1 \Omega$, and placed in the cavity used for the measuring cell. The EJP 30 power supply, purchased from SETARAM, functions as multiple range intensiostat and therefore feeds into the reference cell a precisely determined electrical intensity. The time is determined with an ordinary stopclock.

The heat emitted in the resistor, RI^2t , divided by the area under the recorded curve, yields the calibration constant in cal/cm^2 . The results are given in Table 9.

TABLE 9
CALIBRATION CONSTANTS OF CRMT
CALORIMETER AT 25°

Sensitivity of recorder in mv	0.25	0.50	1.0	2.5	5.0	10.0
$10^3 \times$ Heat/surface in cal/cm^2	3.63	7.38	14.9	37.9	76.0	161.0

3.2.1.6 Source of Errors, Precision and Accuracy

The sources of errors, discussed in section 3.1.1.6, will be found with this calorimeter. In addition, the CRMT model being a monocell calorimeter, the reproducibility is expected to be diminished because of the temperature fluctuations of the metal block (the room in which the calorimeter was housed was well insulated, but not air-conditioned). However, the reproducibility was good, as seen from the self-consistency of the experimental results. Surprisingly, the accuracy was found good also, by testing the calorimeter with a well known system, n-hexane+cyclohexane, which is now

recommended⁷⁷ as the reference system instead of the system $\text{CCl}_4 + \text{Benzene}$. Each cell has been used for that test. The results are given in Figure 15. The accuracy is shown on the respective graphs by the error bars.

3.2.2 Results and Discussion

The heats of mixing of the system iso-C16+n-pentane have been determined at 25.0° over a wide concentration range. The results are given in Figure 16, where the heat of mixing per unit "hard core" volume, $\Delta H / (x_1 V_1^* + x_2 V_2^*)$ in cal/cm^3 , is plotted against the segment fraction ϕ_2 of iso-C16. The parameters required for the calculation of the co-ordinates are listed in Table 10. The surface to volume ratios of the normal alkanes, assumed to be cylinders, were calculated according to the Flory recipe³⁰. The same shape was assumed for iso-C16, the radius being taken equal to the radius of PIB, i.e. 3.48 \AA^{14b} . Next, the length of the cylinder was calculated from the reduction volume, V^* , and the surface as well. The 2,2,4-trimethylpentane and 2,2-dimethylbutane were assumed to be spherical, along with benzene and carbon tetrachloride.

It is already remarkable that the heats of mixing of iso-C16+n-pentane are negative. The enthalpy parameter, χ_H , was calculated from the heats of mixing per unit volume according to eq. (41):

FIGURE 15

THE HEAT OF MIXING PER MOLE OF CYCLOHEXANE+
n-HEXANE AS A FUNCTION OF THE MOLAR FUNCTION
OF CYCLOHEXANE AT 25°

open circles: V.T. LAM (ref. 59)
filled circles: BENSON ET AL. (ref. 78)
open squares: OUR DATA

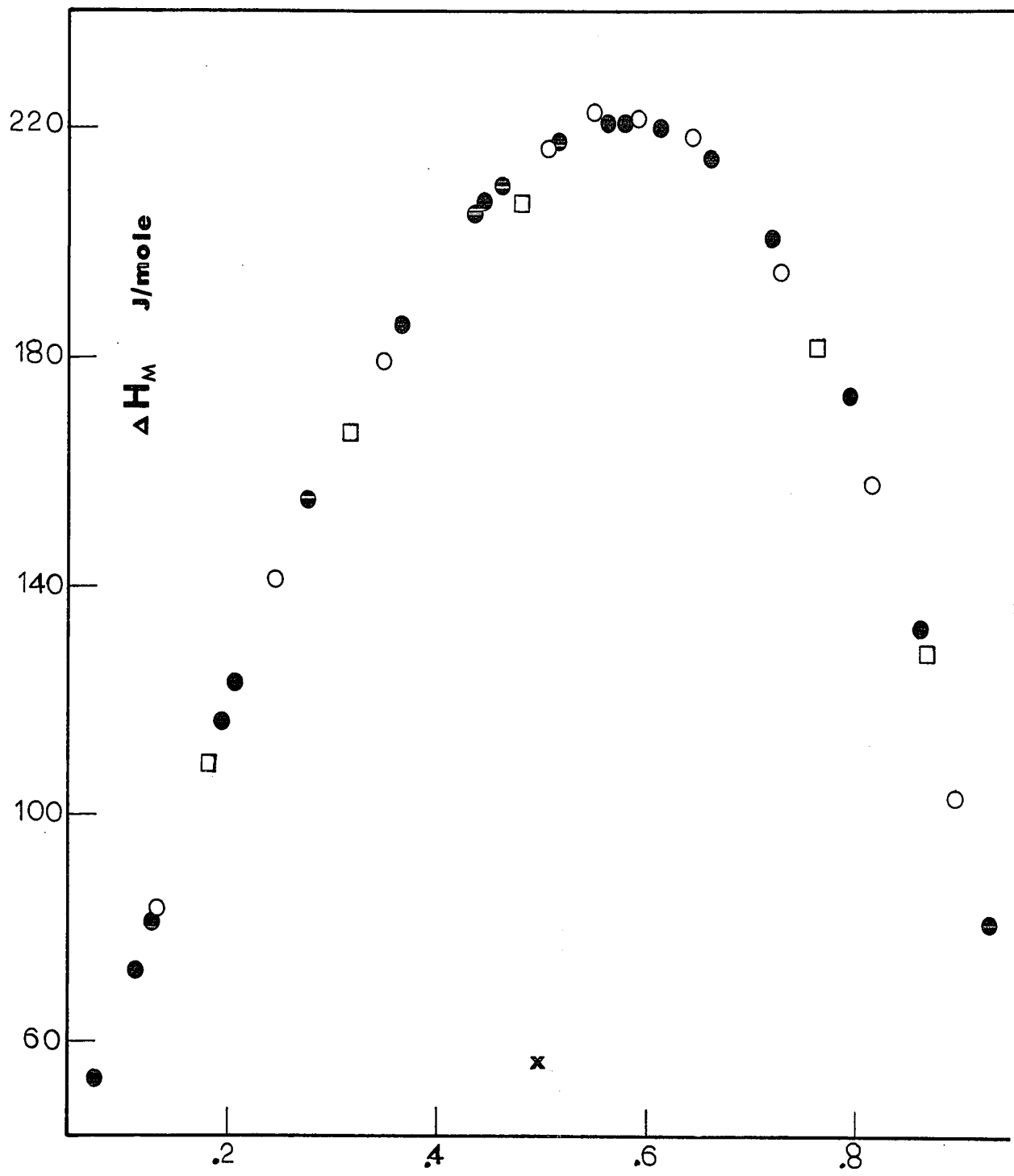


FIGURE 16

THE HEAT OF MIXING PER UNIT "HARD CORE" VOLUME,
 $\Delta H/x_1V_1^* + x_2V_2^*$, AS A FUNCTION OF THE SEGMENT
FRACTION, ϕ_2 , OF ISO-C16* IN n-PENTANE,
AT 25°

* 2,2,4,4,6,8,8-heptamethylnonane

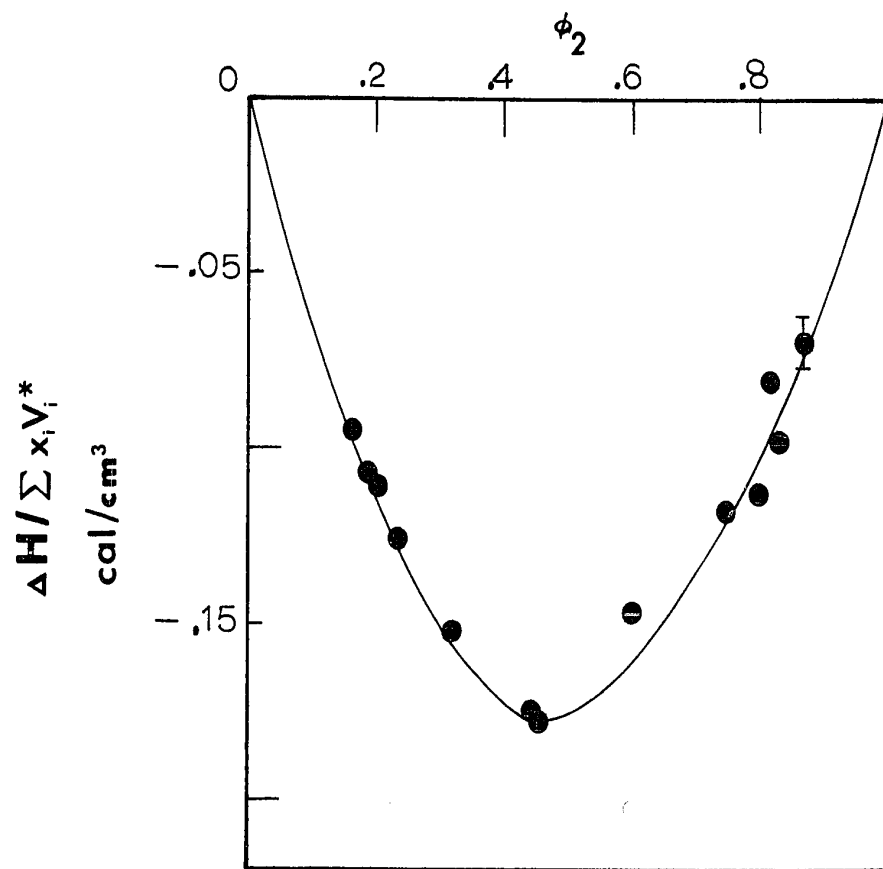


TABLE 10
PURE COMPONENT PARAMETERS AT 25°

LIQUID	v_{sp} (cm ³ /g)	$\alpha \times 10^3$ (deg ⁻¹)	v_{sp}^* (cm ³ /g)	P^* (cal/cm ³)	T^* (°K)	$\frac{\text{surface}}{\text{volume}} (\text{\AA}^{-1})$
2,2,4,4,6,8,8- heptamethylnonane	1.279 (2)	0.8545(2)	1.0513	110.7*	5725	0.768
n-hexadecane	1.2988(1)	0.901 (7)	1.0586	110.7(7)	5549	0.900
2,2,4-trimethyl- pentane	1.4540(1)	1.197 (8)	1.1297	88.3(2)	4756	0.808
n-octane	1.4317(1)	1.159 (7)	1.1194	103.5(7)	4837	0.985
2,2-dimethyl- butane	1.5517(1)	1.472 (2)	1.1606	90.6(2)	4320	0.880
n-hexane	1.5272(1)	1.385 (7)	1.1548	101.2(7)	4434	1.038
n-pentane	1.6094(3b)	1.61 (3b)	1.1830	97.1(3b)	4158	0.927
benzene	1.1444(4)	1.223 (4)	0.8861	150.0(3a)	4709	0.995
carbon tetra- chloride	0.6311(5)	1.229 (6)	0.4882	136.0(6)	4698	0.968

(1) ref. 79; (2) ref. 80; (3a) ref. 14a; (3b) ref. 14d; (4) ref. 81; (5) ref. 82;
(6) ref. 83; (7) ref. 30; (8) ref. 84.

P^* for iso-C16 is not known and was taken equal to the reduction pressure of n-hexadecane.

$$\frac{\Delta H_M}{x_1 V_1^* + x_2 V_2^*} = RT \frac{\chi_H \phi_1 \phi_2}{V_1^*} \quad (41)$$

The results are given in Table 11, and show that χ_H is surprisingly constant over the whole concentration range, the segment fraction varying from 0.16 to 0.83, and equal to -0.10. This is precisely the value found by Kao and co-workers³⁹ for the system PIB+n-pentane (Figure 14c). Comparatively to iso-C16, PIB should give, in n-pentane, a substantially lower negative heat, due to a smaller value of the thermal expansivity of PIB, giving rise therefore to a larger, negative equation of state term in the χ_H expression.

The expression derived by Patterson and Delmas⁵⁰ (their eq. (19)) for the mixing functions, was used in conjunction with the Flory model

$$\tilde{U} = -\tilde{V}^{-1} \quad (42)$$

to calculate the interaction parameter χ_{12} from the heat of mixing. The results are shown in Table 11, and it is seen that the values are constant and small. This reflects the chemical similarity of pentane and the branched nonane. On the other hand, the χ_{12} values obtained for PIB+n-pentane are larger and overestimate the chemical difference between those two components. This is probably due to the procedure by which the χ_{12} was calculated and which involves a fitting

TABLE 11
 EXPERIMENTAL DATA AND CALCULATED PARAMETERS FOR
 THE SYSTEM 2,2,4,4,6,8,8-HEPTAMETHYLNONANE+N-
 PENTANE AT 25°

ϕ_2	ΔH_M (cal/mole)	$\Delta H/\sum x_i V_i^*$ (cal/cm ³)	χ_{12} (cal/cm ³)	χ_H
0.87	-13.29	-0.069	0.20	-0.09
0.83	-17.93	-0.097	0.10	-0.10
0.81	-14.46	-0.081	0.27	-0.08
0.81	-15.82	-0.089	0.23	-0.08
0.80	-19.97	-0.114	0.10	-0.10
0.75	-19.40	-0.118	0.20	-0.09
0.60	-20.12	-0.144	0.27	-0.09
0.46	-21.33	-0.176	0.21	-0.10
0.32	-16.33	-0.152	0.27	-0.10
0.23	-12.61	-0.125	0.31	-0.10
0.20	-10.79	-0.110	0.34	-0.10
0.19	-10.49	-0.107	0.32	-0.10
0.16	- 9.13	-0.096	0.35	-0.10

ϕ_2 is the segment fraction of iso-C16; χ_{12} , the energetic interaction parameter, was calculated by using eq. (19) of ref. 50; χ_H represents the enthalpy parameter and was calculated with eq. (41) from our experimental calorimetric determinations reported in column 2 of this Table.

TABLE 12
EXPERIMENTAL DATA AND CALCULATED PARAMETERS AT 25°

ϕ_2	ΔH_M (cal/mole)	$\Delta H / \sum_i x_i V_i^*$ (cal/cm ³)	X_{12} (cal/cm ³)	X_H
<u>CCl₄+iso-C16</u>				
0.86	72.33	0.397	3.60	0.41
0.86	75.28	0.413	3.73	0.43
0.83	79.71	0.459	3.58	0.41
0.60	93.85	0.732	3.58	0.39
0.59	93.11	0.738	3.58	0.39
0.44	65.38	0.610	3.06	0.31
0.30	58.69	0.620	3.66	0.37
0.22	30.39	0.343	2.61	0.25
0.19	38.23	0.442	3.66	0.36
0.18	37.02	0.431	3.69	0.37
0.16	32.97	0.390	3.71	0.37
0.16	32.47	0.384	3.63	0.36
<u>CCl₄+2,2,4-trimethylpentane</u>				
0.84	62.59	0.539	4.02	0.52
0.82	68.61	0.599	4.02	0.52
0.82	68.35	0.596	4.04	0.52
0.78	78.05	0.700	4.03	0.52
0.59	95.52	0.959	4.06	0.50
0.41	78.52	0.867	3.80	0.45
0.22	56.11	0.678	4.35	0.50
0.17	46.28	0.571	4.40	5.51
0.16	41.19	0.513	4.33	0.50
<u>CCl₄+2,2-dimethylbutane</u>				
0.77	56.72	0.609	3.42	0.44
0.58	76.52	0.872	3.59	0.45
0.57	73.51	0.841	3.44	0.43
0.42	57.16	0.681	2.86	0.35
0.22	45.86	0.578	3.56	0.43
0.21	46.67	0.588	3.63	0.44

TABLE 12 (cont'd)

ϕ_2	ΔH_M (cal/mole)	$\Delta H / \sum_i x_i V_i^*$ (cal/cm ³)	X_{12} (cal/cm ³)	χ_H
<u>Benzene+iso-C16</u>				
0.86	212.19	1.989	10.29	1.15
0.83	228.52	1.355	10.14	1.13
0.80	247.03	1.547	10.19	1.12
0.73	285.41	1.977	10.87	1.18
0.59	253.79	2.130	9.84	1.03
0.54	396.60	3.524	15.83	1.66
0.54	186.51	1.657	7.63	0.78
0.23	120.74	1.463	10.13	0.97
0.19	104.74	1.311	10.53	1.01
0.16	98.68	1.259	11.25	1.07

For symbols, see Table 11

of the heats. Therefore the large X_{12} values reflect merely the overestimation of the free volume term in the theoretical expressions of the mixing functions.

Accordingly, the X_{12} value found for the iso-C16+n-pentane was used for PIB+n-pentane, and a more negative prediction is obtained for χ_H versus ϕ_2 , as shown by curve (2) of Figure 14c. There remains, however, a striking difference between the free volume theories predictions (curve (2) of Figure 14c) and the experimental data (broken line on this graph); a positive heat contribution might reconcile theory and experiment. Moreover, the compensating effect, which is believed to be involved here, would have to have a different concentration dependence from the "interaction" term and the "equation of state" term.

There has been experimental evidence, that order exists in chain-molecule liquids, and particularly in long n-alkanes, as evidence by Bothorel's work,⁸⁶ and which will be discussed later. The disruption of such a structure in the PIB would be an endothermic phenomenon and could explain our results. This led us into a systematic study of heats of mixing of systems containing molecules which might be able to perturb order in a solution, such as carbon tetrachloride.

In Figures 17a, 17b and 18a, the heats of mixing per volume as a function of concentration are given for various systems: CCl₄+iso-C16, +2,2,4-trimethylpentane, +2,2-dimethyl-

FIGURE 17

THE HEAT OF MIXING PER UNIT "HARD CORE" VOLUME,
 $\Delta H/x_1V_1^* + x_2V_2^*$, AS A FUNCTION OF THE SEGMENT
FRACTION, ϕ_2 , OF THE ALKANE, AT 25° FOR

- a) CCl_4 +2,2-dimethylbutane (open circles),
+n-hexane (solid line).⁸⁵
- b) CCl_4 +2,2,4-trimethylpentane (open circles),
+n-octane (solid line).⁸⁵

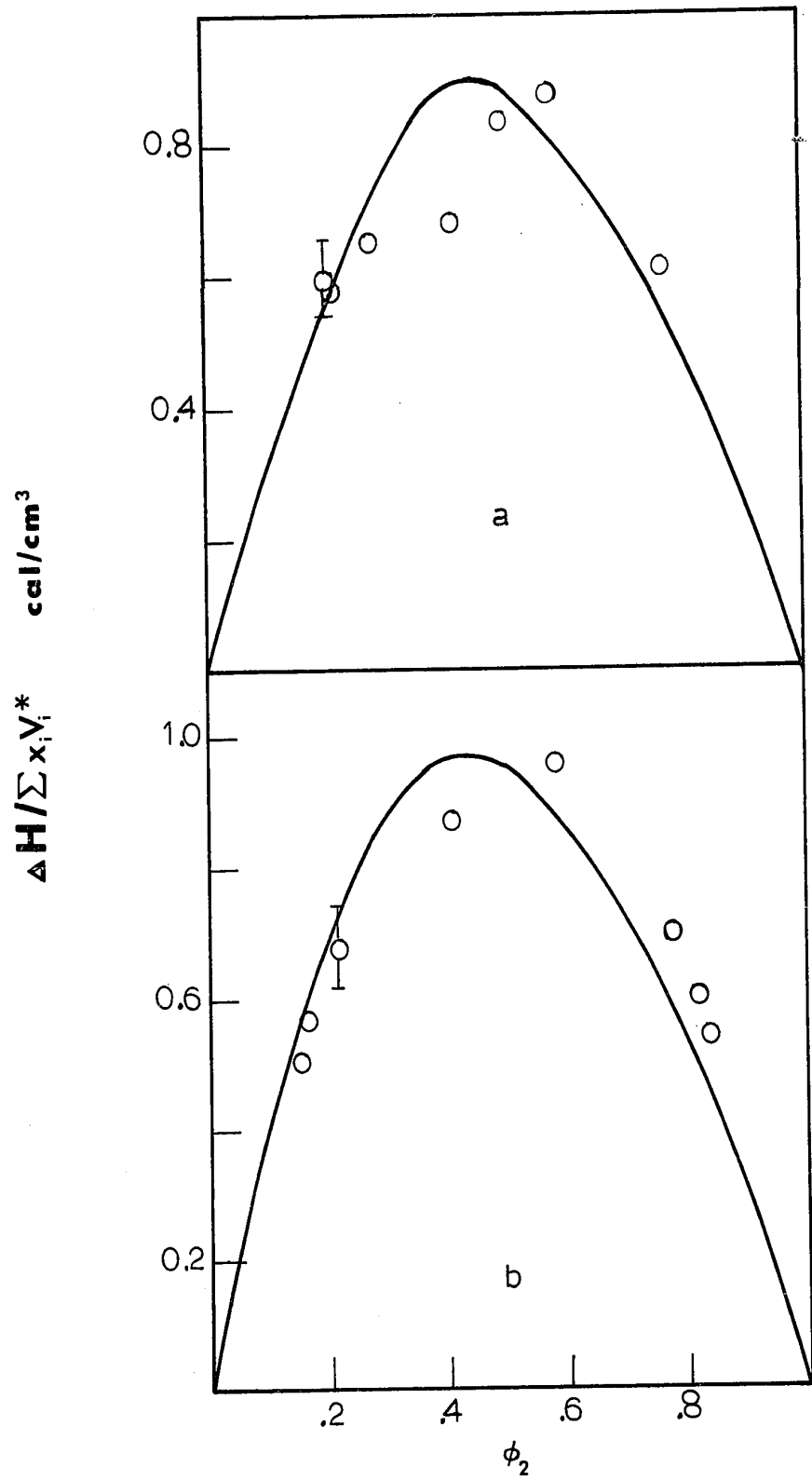
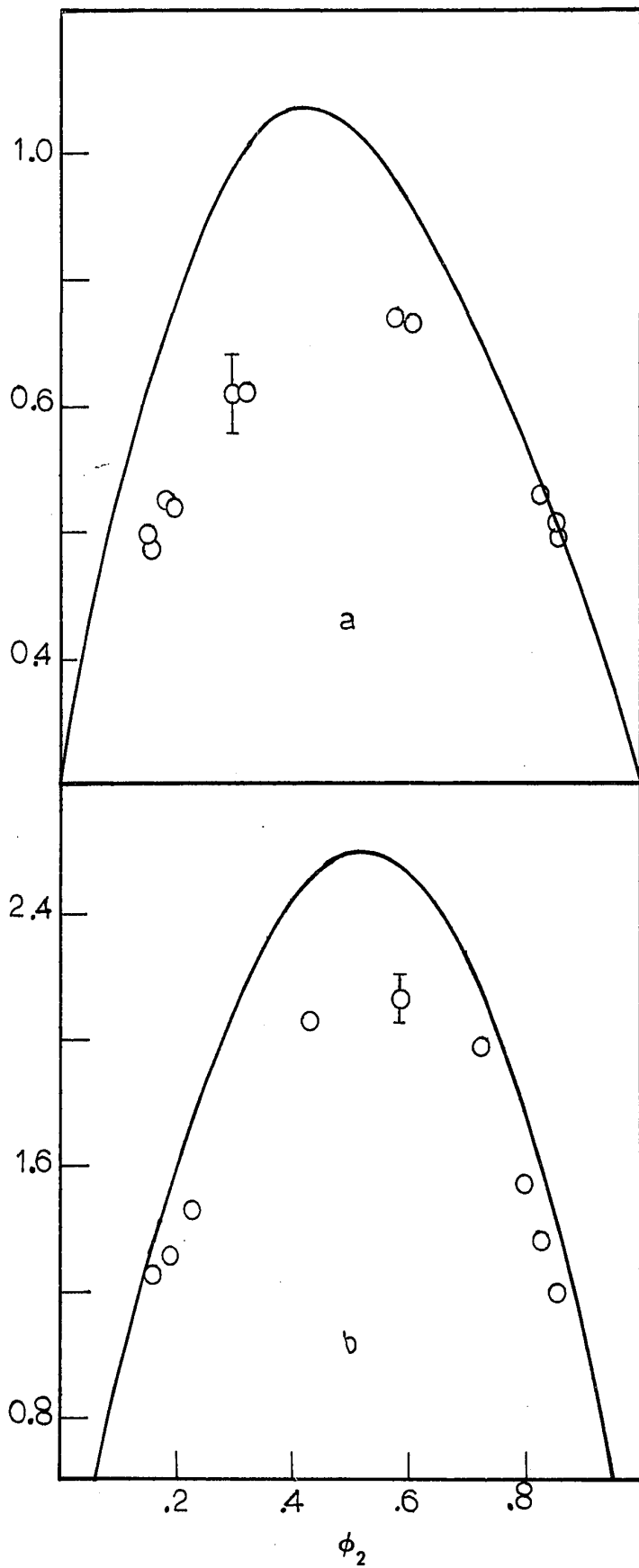


FIGURE 18

THE HEAT OF MIXING PER UNIT "HARD CORE" VOLUME, $\Delta H/x_1$
 $V_1^* + x_2 V_2^*$, AS A FUNCTION OF THE SEGMENT FRACTION,
 ϕ_2 , OF THE ALKANE, AT 25°, FOR

- a) CCl_4 + 2,2,4,4,6,8,8-heptamethylnonane (open circles), +n-hexadecane (solid line).
- b) Benzene+2,2,4,4,6,8,8-heptamethylnonane (open circles), +n-hexadecane (solid line).

$\Delta H / \sum x_i V_i^*$ cal/cm³



butane. In addition, the data for the systems CCl_4 +n-hexadecane, +n-octane, +n-hexane reported by Jain and coworkers⁸⁵, have been treated and reproduced on the respective Figures for comparison purposes with the branched alkanes. The lower alkanes, in C_6 and C_8 , do not show any difference in the heat of mixing, contrary to the iso-C16 and n-C16. For this latter system, the difference is about 0.3 cal/cm^3 at ϕ_2 equal to 0.5, which is equivalent to about 40 cal/mole. In addition, there is a difference in the concentration dependence of the heats of mixing between the normal and the branched alkanes: the maxima are displaced toward higher concentrations (of the alkane) in the case of iso-C16 particularly. Apparently, the n-alkane and especially the n-hexadecane, is able to order more than the iso-C16. This order corresponds to a correlation of orientations of the chains parallel to one another. When the n-hexadecane is mixed with CCl_4 , or another spherical molecule liquid, the order is perturbed and gives rise to a positive heat effect. This would explain our results.

Further evidence for this disordering effect is found by the studies of Bothorel et al.⁸⁶ on alkanes. They measured molecular optical anisotropies, $\langle \gamma^2 \rangle$, by using Depolarized Rayleigh Scattering technique, of normal and branched alkanes in the pure liquid and in dilute solution in carbon tetrachloride and cyclohexane. According to them,

n-hexadecane is particularly ordered, and the order of the n-alkanes is decreased by mixing them with CCl_4 or cyclohexane.

Experimental heats of mixing data of cyclohexane with normal and branched alkanes⁵⁹ show a behaviour similar to the CCl_4 systems we have investigated.

Benzene also can play the role of the disordering molecule. Our results for the system iso-C16+benzene are given in Figure 18b, as well as the data taken from Lundberg⁸⁷. Again, an additional positive heat of 0.5 cal/cm^3 is given off by the normal hexadecane.

The above work shows that a liquid composed of chain-molecules, such as n-hexadecane, has a certain structure or orientational order which is lacking in a liquid composed of spherical molecules. This indicates that these classes of liquids should not obey the same corresponding states laws. The corresponding states principle essentially states that the (configurational) energy, when reduced through division by a suitable parameter, should be the same for all liquids when their free volumes or degrees of thermal expansion are the same. An effect of orientational order is present in the chain-molecule liquids but not in spherical molecule liquids, and only to a limited extent in the mixtures. Thus \tilde{U} might be a different function of \tilde{T} or \tilde{V} for the two classes of liquids and their mixtures. There is much experimental evidence

that high polymers, as well as normal alkanes, display orientational order when they are in the pure state. Studies of strain birefringence of lightly cross-linked networks have provided the best evidence for much order⁸⁸. It seems likely that the thermodynamics of polymer solutions should reflect the presence of order in the polymer and this could be a reason for the failure of the corresponding states principle as applied to polymer solutions. It seems however difficult to reach a definite conclusion here since neither the effect of free volume nor that of order are on a completely firm theoretical basis at present. It appears that further work is necessary before the discrepancies between experiment and the free volume theory can be ascribed to order in the polymer, and not to an inexact free volume term in the theory.

3.3 GENERAL CONCLUSIONS

1. The free volume or equation of state theory of Flory predicts an incorrect concentration dependence of the enthalpy parameter χ_H in solutions where free volume effects are predominant.
2. This failure is not confined to the Flory theory. A general corresponding states approach shows that all theories based on the corresponding states principle for polymers,

solvents and their mixtures would make the same error. The corresponding states principle is therefore called into question.

3. An orientational order of chain-molecules such as n-hexadecane probably exists, and would lead to a failure of the corresponding states principle for solutions of these molecules. A similar orientational order probably exists for high polymers.

4. The χ_H parameter is the same when PIB or a low molecular weight model for PIB is mixed with n-pentane. This indicates that theory overestimates the effect of the very different free volumes of PIB and its low molecular weight model.

5. In view of the probability that the effect of free volume is not properly taken account of by current theory, it is premature to associate the failure of the corresponding states principle in polymer solutions, with an orientational order of the polymer.

4. CONTRIBUTIONS TO ORIGINAL KNOWLEDGE AND
SUGGESTIONS FOR FURTHER WORK

CONTRIBUTIONS TO ORIGINAL KNOWLEDGE

The important results of this work were given in the two sections of this thesis. They are briefly listed below.

1. The technique of light scattering was used to measure properties of polymer solutions under hydrostatic pressure. Therefore, the experimental pressure dependence of thermodynamic parameters could be compared with the predictions of the current free volume theories.

2. Of particular interest to thermodynamics of polymer solutions, are the relative partial molar heat and volume, $\Delta\bar{H}_1$ and $\Delta\bar{V}_1$. According to our results, it seems that fairly accurate values of $\Delta\bar{H}_1$ and $\Delta\bar{V}_1$ may be obtained from light scattering data.

3. In our pressure range, it has been found that the effect on the chain dimensions of a polymer, is similar to that of temperature.

4. A simple "pressure cell" was designed for our light scattering experiments. Although the limit of resistance to internal pressure was about 150 bars, the main advantage of such a cell was the simplicity of use; no special instrumentation or technique is required, the standard SOFICA photogoniometer, which is now used in any research laboratory in polymer science, can be employed without modification for such an investigation.

5. It has been shown that non-solvent systems, such as polystyrene+n-alkanes, may have a negative volume of mixing in the region of the UCST. This unexpected negative value is a contribution from the difference in free volume between the two components.

6. The slope of the critical line, dP/dT , at the UCST has been obtained for a number of systems. Previous work had indicated the effect of pressure on the UCST to be several orders of magnitude less than on the LCST. We have shown here that the dependence of the UCST on pressure can be large.

7. Negative heats of dilution have been obtained, by microcalorimetry, for a number of polymer-solvent systems, which shows the free volume contribution to the enthalpy of dilution. However, the concentration dependence of the enthalpy parameter, χ_H , can not be explained by current free volume theories, and led us to call into question the corresponding states principle, the basis of these theories, as applied to polymer solutions.

8. An order-disorder phenomenon has been observed by calorimetry, in mixtures of long chain alkanes, such as n-hexadecane, and spherical molecules like carbon tetrachloride.

SUGGESTIONS FOR FURTHER WORK

Our work on the pressure dependence of polymer solution properties has been satisfactory, in the sense that theory and experiment are in reasonable agreement for the systems which have been investigated. However, it seems desirable to carry out that type of study at higher pressures, but still using the same technique and equipment (except for the cell). Indeed, of major importance is the effect, if there is one, that pressure would have on the unperturbed dimensions of macromolecules. This was not found in our lower pressure range.

It is in our heat of dilution determinations on polymer solutions, that the shortcomings of corresponding states theories appeared. In the light of our conclusions, two features are of concern:

- we need a more accurate prediction of the free volume contribution to any thermodynamic function which is meant to describe a polymer solution,

- a better understanding and estimation of the orientational order in such solutions.

Heat of dilution determinations on model compound mixtures and polymer solutions at higher temperatures, should provide us with some answers.

This would also eliminate a difficulty to apply free volume theories: the estimation of the "contact interaction" term X_{12} , which is done by fitting a thermodynamic quantity to experiment, and presupposes therefore a most accurate "equation of state" term.

Finally, in conjunction with obtaining chemical potential values from light scattering data, by studying systems under hydrostatic pressure, it might be desirable to measure, by calorimetry, heats of dilution of the same systems under pressure.

REFERENCES

1. H. Tompa, "Polymer Solutions", Butterworth's, London, Academic Press, New York, 1956.
2. A. Morawetz, "Macromolecules in Solution", Interscience Publishers, New York, 1965.
3. P.J. Flory, J. Chem. Phys., 10, 51 (1942).
4. M.L. Huggins, J. Phys. Chem., 46, 151 (1942).
5. P.J. Flory, "Principles of Polymer Chemistry", Cornell University Press, Ithaca, New York, 1953, p. 510.
6. E.A. Guggenheim, Disc. Faraday Soc., 15, 24 (1953).
7. P.I. Freeman and J.S. Rowlinson, Polymer, 1, 20 (1960).
8. G. Delmas, D. Patterson and T. Somcynsky, J. Polymer Sci., 57, 79 (1962).
9. G. Delmas, D. Patterson and D. Bohme, Trans. Faraday Soc., 58, 2116 (1962).
10. I. Prigogine (with the collaboration of V. Mathot and A. Bellemans), "The Molecular Theory of Solutions", North Holland Publishing Co., Amsterdam, 1957.
11. P.J. Flory, Disc. Faraday Soc., 49, 7 (1970).
12. D. Patterson, Macromolecules, 2, 672 (1969).
- 13a. G. Allen and C.H. Baker, Polymer, 6, 181 (1965);
b. L. Zeman, J. Biros, G. Delmas and D. Patterson, J. Phys. Chem., in press.
14. B.E. Eichinger and P.J. Flory, Trans. Faraday Soc., 64, a) 2035; b) 2053; c) 206; d) 2066, (1968).
15. P.J. Flory and H. Hocker, Trans. Faraday Soc., 67, 2258 (1971).
16. H. Hocker and P.J. Flory, *ibid.*, 2270 (1971).

17. H. Hocker, H. Shih and P.J. Flory, *ibid.*, 2275 (1971).
18. G.V. Schulz and M. Lechner, *J. Polymer Sci., Part A-2*, 8, 1885 (1970).
19. M. Lechner and G.V. Schulz, *European Polymer J.*, 6, 945 (1970).
20. G.V. Schulz and M. Lechner in M.B. Huglin, "Light Scattering from Polymer Solutions", Academic Press, New York (1971).
21. D. Patterson and G. Delmas, *Trans. Faraday Soc.*, 65, 708 (1969).
22. B.A. Wolf, *Ber. Bunsen-Ges. Phys. Chem.*, 75, 924 (1971).
23. M. Kurata and W.H. Stockmayer, *Fortschr. Hochpolym. Forsch.*, 3, 196 (1963).
24. J. Pouchly, J. Biros, K. Solc and J. Vondrejsova, *J. Polymer Sci., Part C*, 16, 679 (1967).
25. R. Koningsveld, L.A. Kleintjens and A.R. Shultz, *J. Polymer Sci., Part A-2*, 8, 1261 (1970).
26. C. Wippler and G. Scheibling, *J. Chim. Phys.*, 51, 201 (1954).
27. G. Delmas and D. Patterson, *Polymer*, 7, 513 (1966).
28. G.C. Berry, *J. Chem. Phys.*, 44, 4550 (1966).
29. C.J.F. Bottcher, "Theory of Electric Polarization", Elsevier Publishing Co., 1952.
30. P.J. Flory, J.L. Ellison and B.E. Eichinger, *Macromolecules*, 1, 279 (1968).
31. H.J. Cantow, *Z. Phys. Chem.*, 7, 58 (1956).
32. K.A. Stacey, "Light Scattering in Physical Chemistry", Butterworths, London, 1956.
33. I. Prigogine and R. Defay, "Chemical Thermodynamics", Longmans, London, 1954, p. 289.
34. W.R. Krigbaum, D.K. Carpenter, M. Kaneko and A. Roig, *J. Chem. Phys.*, 33, 921 (1960).

35. E.F. Casassa and H. Markovitz, J. Chem. Phys., 29, 493 (1958).
36. M. Kurata, M. Fukatsu, H. Sotobayashi and H. Yamakawa, J. Chem. Phys., 41, 139 (1964).
37. P.J. Flory and W.R. Krigbaum, J. Chem. Phys., 18, 1086 (1950).
38. C.H. Baker, W.B. Brown, G. Gee, J.S. Rowlinson, D. Stubley and R.E. Yeadon, Polymer, 3, 215 (1962).
39. W.P. Kao, R.E. Chahal and D. Patterson, to be published.
40. G. Allen, G. Gee and G.J. Wilson, Polymer, 1, 456 (1960).
41. A. Dondos and H. Benoit, Macromolecules, 4, 279 (1970).
42. G. Tanaka, S. Imai and H. Yamakawa, J. Chem. Phys., 52, 2639 (1970).
43. H. Yamakawa and M. Kurata, J. Chem. Phys., 32, 1852 (1960).
44. E.F. Casassa, Polymer, 3, 625 (1962).
45. J.S. Ham, M.C. Bolen and J.K. Hughes, J. Polymer Sci., 57, 25 (1962).
46. C. Cuniberti and U. Bianchi, Polymer, 7, 151 (1966).
47. D. Patterson, G. Delmas and T. Somcynsky, Polymer, 8, 503 (1967).
48. A.R. Shultz and P.J. Flory, J. Amer. Chem. Soc., 73, 1909 (1951).
49. K.S. Siow, G. Delmas and D. Patterson, Macromolecules, 5, 29 (1972).
50. D. Patterson and G. Delmas, Disc. Faraday Soc., 49, 1 (1970).
51. G. Lewis and A.F. Johnson, J. Chem. Soc. (A), 1816 (1969).
52. D.W. Dreifus and D. Patterson, Trans. Faraday Soc., 67, 631 (1971).

53. D. Patterson, S.N. Bhattacharyya and P. Picker, *ibid.*, 64, 648 (1968).
54. G.V. Schulz, K.V. Gunner and H. Gerrens, *Z. Phys. Chem. (N.F.)*, 4, 192 (1955).
55. E. Calvet and H. Prat, "Recent Progress in Microcalorimetry", Pergamon Press, New York, 1963.
56. M.A. Kabayama and H. Daoust, *J. Phys. Chem.*, 62, 1127 (1958).
57. M. Senez and H. Daoust, *Can. J. Chem.*, 40, 734 (1962).
58. H. Hocker, G.J. Blake and P.J. Flory, *Trans. Faraday Soc.*, 67, 2251 (1971).
59. V.T. Lam. private communication (1971).
60. W.R. Krigbaum and D.O. Geymer, *J. Amer. Chem. Soc.*, 81, 1859 (1959).
61. Th.G. Scholte, *J. Polymer Sci., Part A-2*, 8, 841 (1970).
62. S. Morimoto, *Makromol. Chem.*, 133, 197 (1970).
63. I.A. McLure, J.E. Bennett, A.E.P. Watson and G.C. Benson, *J. Phys. Chem.*, 69, 2759 (1965).
64. J. Timmermans, "Physico-Chemical Constants of Pure Organic Compounds", Elsevier Publishing Co., New York, 1950.
65. K. Shinoda and J.H. Hildebrand, *J. Phys. Chem.*, 65, 183 (1961).
66. D.E.G. Jones, I.A. Weeks and G.C. Benson, *Can. J. Chem.*, 49, 2481 (1971).
67. G.C. Benson, S. Murakami, V.T. Lam and Jaswant Singh, *Can. J. Chem.*, 48, 211 (1970).
68. P. Outer, C.I. Carr and B.H. Zimm, *J. Chem. Phys.*, 18, 830 (1950).
69. C.E.H. Bawn and M.A. Wajid, *J. Polymer Sci.*, 12, 109 (1954).
70. M.J. Schick, P. Doty and B.H. Zimm, *J. Amer. Chem. Soc.*, 71, 530 (1950).

71. C.E.H. Bawn, R.F.J. Freeman and A.R. Kamaliddin, *Trans. Faraday Soc.*, 46, 677 (1950).
72. A. Kagemoto, S. Murakami and F. Fujishiro, *Bull. Chem. Soc. Japan*, 39, 15 (1966).
73. S.H. Maron and F.E. Filisko, *J. Macromol. Sci.*, B-6, 1, 57 (1972).
74. K. Schmoll and E. Jenckel, *Z. Elektrochem.*, 60, 756 (1956).
75. A. Bondi, *J. Phys. Chem.*, 68, 441 (1964).
76. D. Patterson, *J. Polymer Sci., Part C*, 16, 3379 (1968).
77. M.L. McGlashan and H.F.J. Stoeckli, *J. Chem. Thermodyn.*, 1, 589 (1969).
78. S. Murakami and G.C. Benson, *J. Chem. Thermodyn.*, 1, 559 (1969).
79. American Petroleum Institute, Research Project 44, "Selected Values of Physical and Thermodynamic Properties of Hydrocarbons and Related Compounds", Carnegie Press, Pittsburgh, Pa., 1953.
80. J.M. Bardin, Thesis, McGill University, Montreal (1972).
81. S.E. Wood and J.P. Brusie, *J. Amer. Chem. Soc.*, 65, 1891 (1943).
82. S.E. Wood and J.A. Gray, *ibid.*, 74, 3729 (1952).
83. A. Abe and P.J. Flory, *ibid.*, 82, 1838 (1965).
84. S.E. Wood and O. Sandus, *J. Phys. Chem.*, 60, 801 (1956).
85. D.R.S. Jain, O.P. Yadav and S.S. Gill, *Ind. J. Chem.*, 9, 339 (1971).
- 86a. C. Clement and P. Bothorel, *J. Chim. Phys.*, 66, 878 (1964);
b. P. Bothorel, *J. Coll. Interface Sci.*, 27, 529 (1968).
87. G.W. Lundberg, *J. Chem. Eng. Data*, 9, 193 (1964).
88. T. Ishikawa and K. Nagai, *Polymer J.*, 1, 116 (1970).

APPENDIX

TABLES OF SUPPORTING DATA FOR FIGURES

FIGURE 2, Page 23

$c \times 10^2$ (g/cm ³)	$\Delta n \times 10^3$
1.070	2.018
0.616	1.227
0.356	0.667
0.285	0.539
0.116	0.219

FIGURES 3 and 4, Pages 27 and 28

PIB+2-Methylbutane

P (bar)	T ⁰	$\langle S^2 \rangle^{\frac{1}{2}}$ (Å)			$A_2 \times 10^4$ (cm ³ moleg ⁻²)		
		24	57	64	24	57	64
0	338	300	-	-	0.71	-0.46	-
30	364	300	300	300	0.99	-0.05	-0.45
60	384	318	325	325	1.24	0.45	0.12
90	390	359	378	378	1.45	0.80	0.70
110	382	380	355	355	1.58	1.13	0.90

PS+2-Butanone at 22°

P (bar)	$A_2 \times 10^4$ (cm ³ mole g ⁻²)	$\langle S^2 \rangle^{\frac{1}{2}}$ (Å)
0	1.08	335
40	1.24	340
80	1.30	367
110	1.64	374

FIGURE 6, Page 42

$C \times 10^5$ (g/cm ³)	<u>45</u>	<u>60</u>	<u>75</u>	<u>90</u>	<u>105</u>	<u>120</u>	<u>135</u>
$C_1 = 194.1$	1.465	1.500	1.550	1.595	1.650	1.685	1.725
$C_2 = 150.2$	1.365	1.405	1.460	1.500	1.555	1.590	1.630
$C_3 = 125.1$	1.305	1.340	1.390	1.440	1.490	1.530	1.575
$C_4 = 97.5$	1.250	1.285	1.335	1.380	1.435	1.470	1.510
$C_5 = 67.0$	1.180	1.215	1.265	1.310	1.360	1.395	1.430
$C_6 = 36.4$	1.115	1.150	1.200	1.245	1.290	1.325	1.360

FIGURE 8, Page 51

<u>System</u>	<u>P</u> <u>(bar)</u>	<u>T</u> <u>(°C)</u>
PS+n-hexane	260	8.
	100	13.
	80	15.
	0	19.
PS+n-octane	95	26.
	60	27.
	8	28.
PS+n-dodecane	200	27.
	95	28.
	8	28.
PS+n-hexadecane	320	28.5
	0	29.
PS+2,2-dimethylbutane	210	13.
	174	13.5
	130	15.5
	68	18.5
	0	21.5

FIGURE 10, Page 54

M_2	2,030	4,000	10,000	2,030	4,000	10,000
$T_c(^{\circ}C)$	17.5	31.0	71.5	224.	200.	= 155.
r	14.5	28.4	68.1	10.2	20.6	59.5
$\frac{1}{r^{\frac{1}{2}}} + \frac{1}{2r}$	0.30	0.20	0.13	0.36	0.24	0.14
$\frac{1}{T_c} \times 10^3$	3.44	3.30	2.90	2.01	2.07	2.34

FIGURE 13, Page 69

M_2	Δn_1 (mole)	ϕ_2^i	ϕ_2^f	ϕ_2^a	ΔH_d (cal)	x_H
<u>PS+CYCLOHEXANE</u>						
600	0.0247	0.738	0.667	0.70	5.61	0.89
	0.0456	0.667	0.554	0.61	8.42	0.83
	0.0493	0.554	0.457	0.51	5.90	0.79
	0.0586	0.457	0.364	0.41	4.47	0.76
	0.0559	0.239	0.191	0.22	1.17	0.76
	0.0569	0.142	0.114	0.13	0.44	0.69
	0.0567	0.082	0.066	0.07	0.11	0.63
2100	0.0522	0.427	0.346	0.39	2.99	0.64
	0.0526	0.346	0.281	0.31	1.89	0.61
	0.0561	0.281	0.223	0.25	1.24	0.59
	0.0549	0.223	0.178	0.20	0.81	0.62
	0.0538	0.178	0.142	0.16	0.41	0.50
	0.0533	0.142	0.115	0.13	0.26	0.49
	0.0550	0.115	0.092	0.10	0.17	0.49
	0.0551	0.092	0.073	0.08	0.11	0.52
20,400	0.0536	0.283	0.229	0.26	1.02	0.49
	0.0542	0.229	0.184	0.21	0.59	0.43
	0.0525	0.184	0.149	0.17	0.40	0.46
	0.0498	0.149	0.122	0.14	0.24	0.44
	0.0497	0.122	0.099	0.11	0.16	0.45
	0.0506	0.099	0.081	0.09	0.12	0.49
<u>PS+CYCLOPENTANE</u>						
600	0.0397	0.755	0.652	0.70	5.61	0.48
	0.0408	0.652	0.560	0.61	4.28	0.48
	0.0615	0.560	0.456	0.51	3.97	0.42
	0.0695	0.456	0.367	0.41	1.99	0.32
	0.0625	0.367	0.296	0.33	1.64	0.40
	0.0645	0.159	0.126	0.14	0.28	0.36
	0.0385	0.419	0.341	0.38	1.35	0.41
2100	0.0689	0.495	0.368	0.43	2.92	0.39
	0.0682	0.368	0.290	0.33	1.55	0.35
	0.0670	0.290	0.233	0.26	0.88	0.32
	0.0657	0.233	0.185	0.21	0.54	0.32
	0.0634	0.161	0.129	0.14	0.25	0.32
	0.0661	0.095	0.076	0.09	0.08	0.30

FIGURE 13, Page 69

M_2	Δn_1 (mole)	ϕ_2^i	ϕ_2^f	ϕ_2^a	ΔH_d (cal)	x_H
<u>PS+2-BUTANONE</u>						
2100	0.0677	0.559	0.450	0.50	-0.29	-0.03
	0.0679	0.450	0.354	0.40	-0.17	-0.03
	0.0667	0.354	0.284	0.32	-0.15	-0.04
	0.0705	0.284	0.224	0.25	-0.09	-0.04
	0.0720	0.298	0.235	0.27	-0.13	-0.05
	0.0670	0.604	0.467	0.54	-0.19	-0.02
10,000	0.0698	0.362	0.264	0.31	-0.13	-0.03
	0.0702	0.264	0.205	0.24	-0.05	-0.02
	0.0678	0.205	0.163	0.18	-0.07	-0.05
51,000	0.0722	0.217	0.160	0.19	-0.08	-0.05
	0.0705	0.160	0.123	0.14	-0.03	-0.04
97,000	0.0709	0.244	0.181	0.22	-0.05	-0.02
	0.0711	0.181	0.141	0.16	-0.02	-0.02

FIGURE 14, Page 70

M_2	Δn_1 (mole)	ϕ_2^i	ϕ_2^f	ϕ_2^a	ΔH_d (cal)	x_H
<u>PS+TOLUENE</u>						
600	0.0590	0.532	0.423	0.48	-1.17	-0.15
	0.0609	0.423	0.333	0.38	-0.71	-0.14
	0.0600	0.333	0.263	0.30	-0.44	-0.14
	0.0605	0.263	0.207	0.24	-0.26	-0.13
	0.0604	0.207	0.163	0.19	-0.17	-0.14
	0.0606	0.163	0.128	0.15	-0.09	-0.12
	0.0601	0.128	0.101	0.11	-0.05	-0.12
	0.0609	0.101	0.079	0.09	-0.03	-0.12
	0.0610	0.679	0.062	0.07	-0.02	-0.13
	0.0607	0.049	0.039	0.04	-0.01	-0.10
2030	0.0565	0.304	0.235	0.27	-0.33	-0.14
	0.0566	0.156	0.122	0.14	-0.11	-0.17
2100	0.0568	0.513	0.408	0.46	-1.60	-0.22
	0.0575	0.408	0.327	0.37	-0.88	-0.19
	0.0574	0.327	0.262	0.30	-0.51	-0.17
	0.0551	0.262	0.211	0.24	-0.26	-0.14
	0.0564	0.211	0.167	0.19	-0.17	-0.14
	0.0551	0.167	0.134	0.15	-0.10	-0.14
	0.0558	0.134	0.107	0.12	-0.06	-0.13
20,400	0.0390	0.437	0.370	0.40	-0.64	-0.17
	0.0576	0.370	0.292	0.33	-0.58	-0.16
	0.0578	0.292	0.233	0.26	-0.26	-0.11
	0.0573	0.233	0.185	0.21	-0.18	-0.12
	0.0556	0.185	0.148	0.17	-0.10	-0.12
	0.0581	0.148	0.118	0.13	-0.05	-0.08
<u>PS+ETHYLBENZENE</u>						
2100	0.0480	0.558	0.439	0.50	-0.45	-0.06
	0.0518	0.439	0.337	0.39	-0.30	-0.06
	0.0511	0.397	0.259	0.30	-0.15	-0.06
	0.0499	0.259	0.199	0.23	-0.08	-0.06
	0.0522	0.199	0.152	0.18	-0.04	-0.05
	0.0506	0.152	0.116	0.13	-0.01	-0.03
	0.0460	0.309	0.228	0.27	-0.11	-0.06
	0.0499	0.298	0.174	0.20	-0.06	-0.06
	0.0502	0.174	0.134	0.15	-0.03	-0.04
	0.0518	0.134	0.101	0.12	-0.01	-0.04
	0.0501	0.101	0.077	0.09	-0.01	-0.04

FIGURE 15, Page 93

<u>X</u> <u>(molar fraction of</u> <u>cyclohexane)</u>	<u>ΔH_M</u> <u>(J/mole)</u>
0.18	108.8
0.32	167.0
0.47	206.0
0.76	180.8
0.87	128.5